

# Low temperature rotational relaxation of CO in self-collisions and in collisions with Ne and He

G. A. Amaral<sup>a</sup>, F. J. Aoiz<sup>a</sup>, L. Bañares<sup>a</sup>, J. Barr<sup>a,+</sup>, V. J. Herrero<sup>b,\*</sup>, B.  
Martínez-Haya<sup>c,\*</sup>, M. Menéndez<sup>a</sup>, G. A. Pino<sup>a,#</sup>, I. Tanarro<sup>b</sup>, I. Torres<sup>a</sup>, J. E.  
Verdasco<sup>a</sup>

<sup>a</sup>Departamento de Química Física. Facultad de Química, Universidad Complutense de  
Madrid, E-28040 Madrid, Spain

<sup>b</sup> Instituto de Estructura de la Materia (CSIC), Serrano 123, E-28006 Madrid, Spain

<sup>c</sup> Departamento de Ciencias Ambientales, Universidad Pablo de Olavide, E-41013  
Sevilla, Spain

<sup>+</sup> Present address: Instituto Catalán de Investigaciones Químicas, Av. Paisos Catalans,  
s/n, 43007 Tarragona, Spain.

<sup>#</sup> Present address: Departamento de Fisicoquímica. Facultad de Ciencias Químicas.  
Universidad de Córdoba. 5000 Córdoba. Argentina.

\* Corresponding authors: [vherrero@iem.cfmac.csic.es](mailto:vherrero@iem.cfmac.csic.es), [bmarhay@upo.es](mailto:bmarhay@upo.es)

## Abstract

The low temperature rotational relaxation of CO in self collisions and in collisions with the rare gas atoms Ne and He has been investigated in supersonic expansions with a combination of resonance-enhanced-multiphoton ionization (REMPI) spectroscopy and time-of-flight techniques. For the REMPI detection of CO, a novel 2+1' scheme has been employed through the A<sup>1</sup>Π state of CO. From the measured data, average cross-sections for rotational relaxation have been derived as a function of temperature in the range 5-100 K. For CO-Ne and CO-He, the relaxation cross-sections grow, respectively, from values of  $\approx 20$  and  $7 \text{ \AA}^2$  at 100 K, to values of  $\approx 65-70 \text{ \AA}^2$  and  $\approx 20 \text{ \AA}^2$  in the 5-20 K temperature range. The cross-section for the relaxation of CO-CO grows from a value close to  $40 \text{ \AA}^2$  at 100 K to a maximum of  $60 \text{ \AA}^2$  at 20 K and then decreases again to  $40 \text{ \AA}^2$  at 5 K. These results are qualitatively similar to those obtained previously with the same technique for N<sub>2</sub>-N<sub>2</sub>, N<sub>2</sub>-Ne and N<sub>2</sub>-He collisions, although in the low temperature range (T < 20 K) the CO relaxation cross sections are significantly larger than those for N<sub>2</sub>. Some discrepancies have been found between the present relaxation cross sections for CO-CO and CO-He and the values derived from electron induced fluorescence experiments.

## 1. Introduction

Low temperature rotational energy transfer in CO molecules plays an important role in many interstellar environments (see for instance refs 1-3 and references therein). On the other hand, CO is a relatively light diatomic molecule, isoelectronic with nitrogen but possessing a dipole moment, and thus an interesting subject for a basic study of intermolecular interactions and collisional processes with other light partners.

A wealth of experimental methods has been applied to the investigation of the rotational energy transfer of CO in self collisions and in collisions with rare-gas (Rg) atoms. These methods include sound absorption,<sup>4-5</sup> thermal conduction and diffusion measurements,<sup>6-9</sup> broadening and shifting of spectral lines,<sup>10-20</sup> and the application of electron induced fluorescence and diverse laser techniques, sometimes under bulk conditions,<sup>21-23</sup> but mostly in combination with supersonic expansions or molecular beams.<sup>24-34</sup> Since the mid 1990s, different spectroscopic studies of the CO-CO and CO-Rg van der Waals complexes have also been performed.<sup>35-44</sup> State resolved cross sections and rate constants for energy transfer have been often deduced from various sorts of experimental data by applying models and scaling laws.<sup>18-23,26</sup> However, the empirical state-to-state rate constants derived from a particular experiment are often ambiguous, depend on the assumptions of the specific model used, and cannot always account for experimental data of another kind (see for instance the discussions in refs 20, 22, 23 and 26). Empirical estimates of total (*i.e.* non-state resolved) cross sections or rate constants, though also approximate, are in general more reliable.

The joint analysis of a large group of experimental properties and the progress in the theoretical methodology over the last decade have provided a series of high quality semiempirical and *ab initio* potential energy surfaces (PESs) for the CO-X systems under consideration in the present work.<sup>45-55</sup> Dynamical calculations on these PESs are producing a set of cross sections and rate constants<sup>3,22,23,27,30,31,54,56-58</sup> that can be used for the simulation of the measurements, which provides a less ambiguous comparison between experiment and theory than the experimental inversion procedures mentioned in the previous paragraph. The accuracy of the calculations is higher for collisions of CO with atomic partners, for which better theoretical methods have been developed.

Experimental data on CO rotational relaxation at low temperature ( $T < 80$  K) have been derived from measurements in supersonic expansions,<sup>26,27,29,33,34</sup> mostly free jets, that are specially suited for the generation of very cold gas phases. The determination of relaxation rate coefficients or cross sections from the analysis of the free jet data requires a description of the supersonic flow, which can, in principle, be obtained from the solution of the hydrodynamic equations,<sup>59</sup> although in practice this is not always feasible. In some cases, a detailed experimental characterization of free jet flow fields is also becoming possible thanks to recent experimental progress.<sup>60-62</sup> In free jet expansions with axial symmetry, such as the ones employed in our work, simple and reliable expressions for the description of the jet axis are available if isentropic behaviour can be assumed, which is often the case (see refs 63 and 64 and references therein).

Another kind of supersonic expansion used for kinetic studies of gases at low temperatures is obtained using the CRESU (Cinétique de Reaction en Ecoulement Supersonique Uniforme) technique.<sup>65,66</sup> This method is based on the use of converging-diverging Laval nozzles instead of free jets, and produces flow fields with constant temperatures over an appreciable region of the expansion. A suitably designed Laval nozzle is needed for each temperature. A combination of these uniform flows with laser techniques can provide very detailed state-selective information on relaxation processes. However, even the most recent CRESU experiments in which both initial and final rotational states of the CO molecules in a constant temperature supersonic flow are analysed,<sup>34</sup> require some degree of modelling for the derivation of experimental cross sections and rate coefficients.

In addition to the refined state-selective measurements, which are in general restricted to a small set of states and collision energies, the experimental estimate of average thermal cross sections,  $\sigma_r(T)$ , provides a most valuable information on overall rotational relaxation at low temperatures. Belikov *et al.*<sup>27,32,33,67-70</sup> used the electron induced fluorescence (EIF) technique to derive state-resolved and thermally averaged cross-sections for the rotational relaxation of diatomic molecules ( $N_2$ , CO) in self-collisions and in collisions with rare-gas atoms. These authors measured rotational temperatures along the axis of free jets and applied a thermal conduction model to couple

translational temperatures and rotational states populations assuming isentropic expansions. The EIF technique, has been widely used for the measurement of rotational temperatures of diatomic molecules in free jets, but the interpretation of its data is not straightforward and has lead sometimes to ambiguous or controversial results (see comments in refs 71-73 and in the references cited therein).

In a systematic series of works,<sup>73-76</sup> our group has applied a combination of resonance-enhanced multiphoton ionisation (REMPI) and molecular beam time-of-flight (TOF) techniques to the investigation of the rotational relaxation in N<sub>2</sub>-N<sub>2</sub>, N<sub>2</sub>-He and N<sub>2</sub>-Ne collisions. In these experiments, terminal rotational and translational temperatures were measured in the molecular beams extracted with a skimmer from the centerline of a series of free jet expansions of either N<sub>2</sub>, and of diluted mixtures of N<sub>2</sub> in the rare gases, and thermal cross sections were derived over the  $\approx$ 5-100 K temperature range by applying a simple thermal conduction model. The cross sections for N<sub>2</sub>-N<sub>2</sub> and N<sub>2</sub>-He were compared with the EIF values of Belikov *et al.*,<sup>68-70</sup> which showed approximate accordance for the N<sub>2</sub>-He results,<sup>76</sup> but a noteworthy disagreement for the N<sub>2</sub>-N<sub>2</sub> rotational relaxation data in the low temperature range<sup>73</sup> (below 20 K), where the EIF cross sections were found to be much larger than ours. In later studies, Montero and co-workers<sup>77-79</sup> used free-jet Raman spectroscopy for the investigation of the rotational-translational state-resolved cross sections in N<sub>2</sub>-N<sub>2</sub> and N<sub>2</sub>-He collisions and also estimated thermally averaged cross sections below 20 K.<sup>77,79</sup> The results for N<sub>2</sub>-He, supported by an accurate close-coupling (CC) quantum mechanical calculation,<sup>79</sup> were in agreement with the previous measurements<sup>70,76</sup> within the experimental uncertainty. In the case of N<sub>2</sub>-N<sub>2</sub>, the Raman cross sections<sup>77,78</sup> were at variance with the large EIF values<sup>68</sup> and corroborated the results from the molecular beam REMPI experiments.<sup>73</sup>

In recent works,<sup>27,32,33</sup> the EIF technique has also been used for the determination of  $\sigma_r(T)$  in free jets of CO and of CO-Rg mixtures. Below 100 K, the EIF thermal rate constants for rotational relaxation in CO-CO collisions were similar in magnitude to those obtained in the earlier EIF experiments<sup>68</sup> on the relaxation of N<sub>2</sub>, showing a rise from 10 Å<sup>2</sup> at 100 K to 100 Å<sup>2</sup> at 20 K. Appreciable differences were found between these cross sections and values from line broadening data,<sup>14,15,80</sup> ultrasound absorption<sup>5</sup> and classical trajectories.<sup>56</sup> In the case of CO-He collisions, the EIF  $\sigma_r(T)$ , determined

between 6 and 140 K, grow from 10 to 50 Å<sup>2</sup> with decreasing temperature and are in good agreement with the results of various theoretical calculations<sup>50,81,82</sup> down to 20 K. Data on terminal rotational and translational temperatures for CO-He supersonic expansions from REMPI, infrared (IR) absorption and molecular beam time-of-flight measurements have also been reported.<sup>26,29,33</sup> In order to compare all these results on a common basis, Belikov *et al.*<sup>33</sup> performed infinite order sudden (IOS) state-resolved rate constant calculations on various potential surfaces. With these values and with other rate constants from the literature,<sup>83</sup> Belikov *et al.*<sup>33</sup> estimated  $\sigma_r(T)$  down to 5 K. The joint analysis of the free jet data and the measured terminal temperatures showed apparent inconsistencies and none of the potentials used in the IOS calculations could account for the whole set of data available. Given the just mentioned disparity in the various  $\sigma_r(T)$  for CO, and the discrepancies between the low temperature EIF results for N<sub>2</sub> and those from other methods, commented on in the previous paragraph, additional investigations of the rotational relaxation of CO with different techniques are timely.

In the present study, we have applied the methodology formerly used<sup>73-76</sup> for N<sub>2</sub> to the study of the rotational relaxation in CO in self-collisions and in collisions with rare gas atoms. Thermally averaged rotational relaxation cross sections in CO-CO, CO-Ne and CO-He collisions have been derived in the  $\approx$ 5-100 K temperature interval. As far as we know, these are the first relaxation cross sections for CO-Ne in this temperature range. The results are discussed and, whenever possible, compared to previous experimental and theoretical works.

## 2. Experimental Section

The experimental set-up used for the present measurements is essentially the same as that employed in our previous investigations on the rotational relaxation of the N<sub>2</sub> molecule<sup>73,75,84</sup> and only the relevant details are given here. Free jets of pure CO, and mixtures of CO diluted in He or in Ne (with calibrated CO mole fractions of 0.12 and 0.10, respectively) were generated in supersonic expansions with a pulsed solenoid-driven valve (General Valve) with an effective diameter,  $d_{\text{eff}}=0.42$  mm ( $\pm$ 10%), a pulse frequency of 10 Hz and a pulse width of 0.5-1 ms. The pulsed source was operated at room temperature,  $T_0$ , and at stagnation pressures,  $p_0$ , covering the appropriate range of the relevant parameter  $p_0 d_{\text{eff}}$  between 0.5 and 100 mbar·cm ( $p_0 d_{\text{eff}}$  is proportional to the

inverse of the Knudsen number). The background pressure in the expansion chamber was kept always in the  $10^{-4}$ - $10^{-5}$  mbar interval by a  $2000 \text{ l s}^{-1}$  oil diffusion pump. Molecular beams were extracted by collimating the central part of the free jets with a skimmer at  $\approx 3$ -5 cm downstream from the nozzle. The molecular beam travelled along an arrangement of inter-connected vacuum chambers towards the analysers. In the detection chambers, pumped with turbomolecular pumps, the pressure was kept in the  $10^{-7}$  mbar range.

Time-of-flight (TOF) distributions of the molecular pulses generated by the narrow (1mm width) slits of a mechanical chopper placed in the chamber behind the skimmer were measured for the CO molecules and for the He and Ne atoms by means of a quadrupole mass spectrometer (QMS). The output of the QMS was sent to a digital scope where it could be adequately processed and stored. Extensive averaging of the TOF spectra (up to 64000 averages) was needed for the weakest expansions. Terminal flow velocities,  $u_{\infty}$ , and parallel translational temperatures,  $T_{||,\infty}$ , for CO, He and Ne were derived from the deconvolution of the TOF spectra with a Maxwellian velocity distribution along the axial (“parallel”) streamline of the jet, superimposed to the flow velocity. The flight path between chopper and detector was 49 cm and the geometric gate function of this chopper was approximated by a Gaussian with a FWHM of 24  $\mu\text{s}$ .

The terminal rotational temperatures,  $T_{r,\infty}$ , of CO were obtained from the fit simulation of the REMPI spectra measured on the different molecular beams.<sup>73,75</sup> For that purpose, the molecular beam interacted with UV laser pulses at 21 cm downstream from the skimmer. The UV laser was focussed with a 25 cm focal length lens and the pulsed valve and the laser pulses were synchronized at a repetition rate of 10 Hz. In a first attempt, we tried to use the 2+2 REMPI scheme, in which the same laser pulse used to excite the initial two-photon transition also ionizes the excited molecules, based on the two-photon resonant excitation of CO to the  $A^1\Pi(v=3)\leftarrow X^1\Sigma^+(v=0)$  transition band, as that used by Smith and co-workers.<sup>29</sup> The required tunable laser radiation around 289 nm was generated in a Nd:YAG pumped dye laser (Continuum NY80-20/ND60) operated with a mixture of rhodamine 590 and 610 optimized to produce a flat output power in the region of interest. The resulting laser pulses were linearly polarized and had time and frequency widths of 6 ns and  $0.1 \text{ cm}^{-1}$  (FWHM), respectively. The

experiments were performed with a power of 2 mJ/pulse, which guaranteed a quadratic dependence of the signal on the photon energy, and the  $\text{CO}^+$  ions formed were detected by means of a time-of-flight mass spectrometer of the Wiley McLaren type provided with a dual microchannel plate. The ion signal was corrected with the square of the laser intensity at each wavelength. A typical 2+2 REMPI spectrum obtained under the experimental conditions indicated above is shown in the top panel of Figure 1 corresponding to an expansion of pure CO at  $p_0 d_{\text{eff}} = 85 \text{ mbar}\cdot\text{cm}$ . As can be seen, by using this 2+2 REMPI scheme, the lines of the spectrum are found to be very broad, even causing that some lines are only barely seen. In order to avoid this problem, a 2+1' REMPI scheme was used in which the two-photon excitation corresponding to the  $A^1\Pi(v=3)\leftarrow X^1\Sigma^+(v=0)$  transition band was carried out with a first photon at  $\approx 289 \text{ nm}$  and the ionization step was carried out with a second nanosecond laser pulse at 220 nm with zero time delay with respect to the excitation laser. The 220 nm laser radiation was produced by frequency-mixing the fundamental and second harmonic of a 532 nm Nd:YAG (Quanta Ray Pro 230) laser-pumped dye laser (Continuum ND60) operating in the wavelength range 620-680 nm. The 220 nm laser was focussed using a 50 cm focal length lens and spatially overlapped with the 289 nm laser beam. The 2+1' REMPI spectrum obtained under the same experimental conditions (pure CO and  $p_0 d_{\text{eff}}=85 \text{ mbar}\cdot\text{cm}$ ) is shown in the middle panel of Figure 1. As can be seen, the different lines of the spectrum appear now to be much narrower than those obtained under the 2+2 REMPI scheme, and the weakest lines are also clearly appreciated. Considering that the CO ionization potential (IP) is 14.014 eV,<sup>85</sup> the 2+1' REMPI scheme described above provides a total energy of 14.22 eV, just above the IP of CO. However, for the 2+2 REMPI scheme a total energy of 17.16 eV is available, which is too high in comparison with the IP of CO. This may be the reason of the broader lines obtained in the REMPI spectrum measured under the 2+2 scheme. The 2+1' REMPI scheme was then adopted in the present work to measure all the CO REMPI spectra.

The procedure for the evaluation of rotational distributions from the CO REMPI spectra is described in detail in ref 73 for the case of  $\text{N}_2$ . In the present case the same procedure was used, employing the two-photon line strength factors of the  $A^1\Pi\leftarrow X^1\Sigma^+$  transition and the spectroscopic constants taken from ref 85. Thus, the REMPI rotational line intensities were corrected with the appropriate two-photon line strengths and were then least-square fitted to a Boltzmann distribution. No significant deviations from



Boltzmann distributions were observed. The simulation of the 2+1' REMPI spectrum shown in the middle panel of Figure 1 is depicted in the bottom panel of that Figure and corresponds to a rotational temperature of 3 K. The agreement found between the measured and simulated spectra is very good. Figure 2 shows the measured 2+1' REMPI spectrum measured for an effusive CO beam and the corresponding simulation with a rotational temperature of 298 K.

### 3. Results and Discussion

The present experiments include REMPI and TOF spectra recorded in expansions of pure CO and of CO diluted in Ne and He. For illustration, Figures 3 and 4 show a typical set of such spectra measured for pure CO, along with the corresponding fit simulations, which in each case provide the terminal rotational and translational temperatures and speeds of CO, respectively. The simulation of the REMPI spectra indicated that a Boltzmann distribution of rotational states could be assumed in all cases and that this assumption was satisfactory within the experimental uncertainty. The time of arrival profiles of the CO molecules could be well reproduced with the “drifting Maxwellian” velocity distribution<sup>63,73</sup> usually assumed for supersonic molecular beams. The Figures illustrate the growing rotational and translational cooling attained with increasing number of collisions (increasing  $p_0d_{\text{eff}}$ ) in the expansion.

The whole set of terminal rotational temperatures,  $T_{r,\infty}$ , translational temperatures,  $T_{||,\infty}$ , and flow speeds,  $u_\infty$ , derived from the REMPI and TOF measurements, is represented in Figure 5 (pure CO expansion), Figure 6 (CO/Ne mixture) and Figure 7 (CO/He mixture). As can be seen, in the three cases the rotational temperatures of CO are systematically higher than the translational temperatures over the whole range of  $p_0d_{\text{eff}}$  values investigated. This clearly indicates that the rotation of the CO molecules is not in thermal equilibrium with the translational degrees of freedom of the expanding gas. Furthermore, in the case of the CO/He mixture (Figure 7) for  $p_0d_{\text{eff}} < 10$  mbar·cm, the terminal translational temperatures of CO are higher and the final flow velocities lower than those of He. These differences in  $T_{||,\infty}$  and in  $u_\infty$  were also observed in our former study of N<sub>2</sub>/He mixtures,<sup>76</sup> and show that the number of collisions of the weakest expansions is not enough to maintain translational equilibrium between the two mixture components when the momentum transfer between them is comparatively inefficient

due to the mass disparity. In addition, it is worth noticing that from the comparison of expansions with similar  $p_0 d_{\text{eff}}$  values, the strongest CO cooling (both translational and rotational) is obtained in the collisions with Ne.

In order to explain the observed behaviour of the terminal temperatures and speeds and to obtain an estimate of the thermally averaged rotational relaxation cross sections of CO in self collisions ( $\sigma_{r,\text{CO-CO}}$ ) and in collisions with Ne ( $\sigma_{r,\text{CO-Ne}}$ ), and He ( $\sigma_{r,\text{CO-He}}$ ), we have employed the thermal conduction treatment used in our previous works.<sup>64,74-76</sup> The whole approach is based on a “sudden freeze” model for the otherwise isentropic expansion, in which the appropriate energy transfer between the translational and rotational degrees of freedom is introduced by means of a best-fit thermal relaxation cross section, as described below. In addition, for the general case of lack of equilibrium between the translational degrees of freedom of the two species of the binary mixture, as observed for CO and He, a translational coupling between the CO molecules and the isentropic thermal bath provided by the rare gas is introduced to account for the different local translational temperatures.<sup>76</sup> With these considerations, the evolution of the relevant temperatures is represented by the following differential equations:

$$\frac{dT_{t,\text{CO}}}{dt} = -\frac{1}{\tau_{c,\text{CO-X}}} (T_{t,\text{CO}} - T_{t,\text{X}}) \quad (1a)$$

$$\frac{dT_{r,\text{CO}}}{dt} = -\frac{1}{\tau_{r,\text{CO-CO}}} (T_{r,\text{CO}} - T_{t,\text{CO}}) - \frac{1}{\tau_{r,\text{CO-X}}} (T_{r,\text{CO}} - T_{t,\text{X}}) \quad (1b)$$

where  $(\tau_{c,\text{CO-X}})^{-1}$  and  $(\tau_{r,\text{CO-X}})^{-1}$  are the characteristic collision frequencies for translational and rotational relaxation, respectively, between CO and the collision partner  $X=\text{Ne}$  or  $\text{He}$ . These collision frequencies are related to the corresponding average cross sections by the expression:

$$(\tau_{m,\text{CO-X}})^{-1} = \left(\frac{8kT_{t,\text{X}}}{\pi}\right)^{\frac{1}{2}} n(1-\chi_{\text{CO}}) \mu_{\text{CO-X}}^{-\frac{1}{2}} \sigma_{m,\text{CO-X}} \quad (2)$$

where  $k$  is Boltzmann’s constant,  $n$  the local density,  $\mu_{\text{CO-X}}$  the reduced mass of the CO-X colliding pair and  $\chi_{\text{CO}}$  the mole fraction of CO in the gas mixture. The subscript

$m=c$  or  $r$  denotes translational (collisional) or rotational relaxation, so that  $\sigma_{c,CO-X}$  and  $\sigma_{r,CO-X}$  are the collision cross sections and the cross sections for rotational relaxation, respectively. In the cases of ideal translational equilibrium in the binary mixture ( $T_{t,CO} = T_{t,X}$ ), only eq 1b applies and the system reduces to:

$$\frac{dT_{r,CO}}{dt} = -\frac{1}{\tau_{r,CO-CO}}(T_{r,CO} - T_t) - \frac{1}{\tau_{r,CO-X}}(T_{r,CO} - T_t) \quad (3)$$

Furthermore, for the pure CO expansions we are left with the simplified equation:

$$\frac{dT_{r,CO}}{dt} = -\frac{1}{\tau_{r,CO-CO}}(T_r - T_t) \quad (4)$$

In the present work we have solved equations system (1) for the analysis of the CO-He expansions, eq 3 for the CO-Ne expansions and eq 4 for the pure CO expansions.

The sudden-freeze expansion model relies on the isentropic (adiabatic-isoenthalpic) treatment of the expanding gas, which in our case is propagated at a given  $p_{0d_{eff}}$  until the experimentally observed translational terminal temperature is reached. Within this expansion model, the terminal speed and translational temperature are given by:<sup>63</sup>

$$u_{\infty,X} \approx S_{\infty,X} \left( \frac{2kT_0}{m_{eff}} \right)^{\frac{1}{2}} \left[ 1 - \frac{\gamma-1}{\gamma} S_{\infty,X}^2 \right]^{-\frac{1}{2}} \quad (5)$$

$$T_{||,\infty,X} \approx T_0 \left[ 1 + \frac{\gamma-1}{\gamma} S_{\infty,X}^2 \right]^{-1} \quad (6)$$

where  $m_{eff} = \chi_{CO} \cdot m_{CO} + \chi_X \cdot m_X$  in eq 5 is the average mass of the binary mixture and  $S_{\infty,X} = u_{\infty,X} / (2kT_{\infty,X} / m_X)^{\frac{1}{2}}$  is the terminal speed ratio of the dominant component of the mixture  $X = CO, Ne$  or  $He$ . Within the sudden freeze model, the terminal speed ratio is typically expressed as:<sup>86</sup>

$$S_{\infty} = \frac{F}{(\text{Kn}_0)^G} \quad (7)$$

where  $F$  and  $G$  are  $\gamma$ -dependent constants and  $\text{Kn}_0$  is the source Knudsen number<sup>63</sup>, given by  $\text{Kn}_0 = \sqrt{2} n_0 d_{\text{eff}} \sigma_{c,0}$ , where  $n_0$  and  $\sigma_{c,0}$  stand for the source number density and collision cross section, respectively. The collision cross section can be approximately expressed as:<sup>63,86</sup>

$$\sigma_{c,0} = \left( \frac{53 C_6}{T_0 k} \right)^{\frac{1}{3}} \quad (8)$$

where  $C_6$  is the isotropic attractive term of the intermolecular potential. The main dependence of the speed ratio on  $\text{Kn}_0$  and thus on the number of collisions is carried by the  $G$  exponent. Within the model of Beijrinck and Verster,<sup>86</sup>  $G$  takes the values 0.545 for  $\gamma = 5/3$  and 0.353 for  $\gamma = 7/5$ . In the present work, we have taken  $F$  and  $G$  as fit parameters and have adjusted them to get a good match to the  $T_{||,\infty,X}$  values measured for the dominant component of the expanding mixture. The fitted  $T_{||,\infty,X}$ , as given by eq 6, as a function of  $p_0 d_{\text{eff}}$  are shown in Figures 5, 6 and 7 (dashed lines). The values of  $C_6$  and those of the  $F$  and  $G$  best fit parameters used in eqs 7 and 8 are listed in Table 1.

Note that the G exponent obtained for the CO case is close to the value predicted by the isentropic sudden-freeze model of Beijrinck and Verster<sup>86</sup> for the expansion of diatomic molecules, and that those for expansions dominated by He or Ne are reasonably close to the value predicted for monoatomic gases. The final flow velocities calculated with eq 5 using the parameters of Table 1 are compared in the upper panels of Figures 5-7 to the values determined from our time-of-flight measurements. In general, the agreement is very good and even for the least favourable case, corresponding to the weakest expansions of the CO-He mixture, the difference between the calculated and measured  $u_{\infty,He}$  is only 8%. All these results support the initial assumption of approximate isentropic behaviour in the supersonic expansions.

For the derivation of the temperature-dependent rotational relaxation cross sections  $\sigma_{r,CO-X}(T)$ , the differential equation system of eq 1, or the simplified versions of eq 3 or eq 4, were integrated numerically for each  $p_{0,eff}$  value along the jet axis until the sudden-freeze point given by eq 7, at which the  $T_{t,X}$  in the model reaches a value consistent with the experimental terminal  $T_{||,\infty,X}$ . At this point, the calculated rotational temperature was compared to the measured  $T_{r,\infty}$ , and  $\sigma_{r,CO-X}(T)$  was varied parametrically until a good fit to the experimental data was obtained. The determination of rotational relaxation cross sections from the analysis of the measurements on the CO/Ne and CO/He mixtures requires the previous knowledge of  $\sigma_{r,CO-CO}(T)$ , and this latter thermal cross section was determined in the first place from the pure CO data. In order to integrate eq 1, it is necessary to introduce the value of the cross section,  $\sigma_{c,CO-He}$ , for collisions between CO and He. In this work, for the calculation of this temperature-dependent cross section, eq 8 has been applied with  $C_{6,CO-He}/k=0.77 \times 10^{43} \text{ K cm}^6$  taken from ref 87. Thus, the integration of eq 1 provides  $T_{||,\infty}$  for CO (dotted line of Figure 7) and it is important to remark that these  $T_{||,\infty,CO}$  values have not been fitted to the points, but are directly obtained from the classical  $\sigma_{c,CO-He}$  expression using  $C_6$  values from the literature. In fact, the good agreement between the calculated curve and the measured data for  $T_{||,\infty,CO}$  lends support to the picture underlying the present model by which not only the rotation, but also the translational motion of CO, coupled to the He cold bath through  $\sigma_{c,CO-He}$ , cannot follow the rapid cooling of the rare gas when the collision frequency becomes too low.

The dependence of the rotational relaxation cross section with temperature was represented by the following expression, introduced in previous works:

$$\sigma_{r,CO-X}(T)=A\times\left(\frac{300}{T}\right)^{B-\left(\frac{C}{T}\right)^D} \quad (9)$$

The terminal rotational temperatures provided by the model are shown in Figs. 5-7 along with the experimental values, whereas the corresponding CO-X rotational relaxation cross sections,  $\sigma_{r,CO-X}(T)$ , built with the best-fit parameters A, B, C and D listed in Table 2, are displayed in Fig. 8.

Figure 8 shows that the temperature dependence of the  $\sigma_{r,CO-CO}$ ,  $\sigma_{r,CO-Ne}$  and  $\sigma_{r,CO-He}$  relaxation cross sections follows a similar qualitative trend as that previously observed for  $N_2$  in our previous works.<sup>74-76</sup> For each CO-X collision pair,  $\sigma_{r,CO-X}(T)$  displays initially a monotonic growth as the temperature decreases from 100 K to values of 15-20 K. At sufficiently low temperature, however, the cross section levels off and shows a maximum, which is especially marked in  $\sigma_{r,CO-CO}$  at  $T\approx 20$  K, and hardly appreciable for  $\sigma_{r,CO-Ne}$  and  $\sigma_{r,CO-He}$ . These two latter cross sections maintain roughly constant values of  $\approx 65-70 \text{ \AA}^2$  and  $\approx 20 \text{ \AA}^2$ , respectively, in the temperature range  $T\approx 5-20$  K, whereas the self relaxation cross section  $\sigma_{r,CO-CO}$  decreases from  $\approx 60 \text{ \AA}^2$  at 20 K to roughly 2/3 of this value at  $T\approx 5$  K. In a previous work,<sup>74</sup> we argued that this change of behaviour at low temperature is probably associated with the reaching of the adiabatic regime of inefficient rotational-translational energy transfer.

Another relevant aspect is that the progression  $\sigma_{r,CO-CO} > \sigma_{r,CO-Ne} > \sigma_{r,CO-He}$  is observed at the higher temperatures covered in our work ( $T > 20$  K), whereas, interestingly, at lower temperatures it is found that  $\sigma_{r,CO-CO} < \sigma_{r,CO-Ne}$ , indicating that CO-Ne collisions become more effective than those between CO molecules for the rotational cooling. Again, as can be seen in Figure 8, this same qualitative behaviour is found in the relaxation of  $N_2$ . It may be tentatively asserted that transitions between rotational levels of the colliding diatomic molecules (rotation-rotation transfer in CO-CO or  $N_2-N_2$

collisions) gain in relative importance at these low temperatures and diminish somewhat the rotational de-excitation caused basically by the rotation-translation energy transfer transitions.

According to our results, the cross sections for rotational relaxation of CO are systematically larger than those of N<sub>2</sub>,  $\sigma_{r,CO-X} > \sigma_{r,N_2-X}$ , with the possible exception of He collisions at temperatures close to 100 K, where they are very similar. In the higher temperature range the difference between the CO and the N<sub>2</sub> cross sections, although always within the mutual experimental uncertainty, is systematic and below  $\approx 20$  K the cross sections for rotational relaxation of CO in self collisions and in collisions with Ne become neatly larger than those for N<sub>2</sub>. This is possibly due, at least in part, to the presence of a small permanent dipole moment in the CO molecule which should give rise to stronger attractive interactions, especially in the case of the larger and thus more polarizable collision partners (CO and Ne). The importance of attractive interactions in inelastic collisions<sup>88</sup> is expected to increase markedly at low temperatures. In addition, the relaxation of N<sub>2</sub> is driven by two-quanta transitions due to the ortho-para symmetry of the molecule and this will make rotation-translation transfer more adiabatic, and thus less likely, in the low temperature limit.

The thermal relaxation cross sections of Figure 8 will be discussed below in relation with other results extracted from various experimental sources and from theoretical calculations by different groups, but before doing so we will compare directly some of the terminal temperatures measured in our laboratory to available literature data. Terminal translational temperatures in supersonic molecular beams of pure CO and of a CO-He mixture (10% in CO) were measured by Bassi *et al.*<sup>26</sup> using the same TOF procedure as in the present work and are compared with our values in Figure 9. The  $T_{\parallel,\infty}$  values for expansions of pure CO are in very good agreement with our data. In the CO/He expansions the measurements by Bassi *et al.*<sup>26</sup> show also a breakdown of the translational equilibrium between CO and He, in qualitative accordance with our results. It can be observed that, whereas their  $T_{\parallel,\infty}$  values for the He seed gas are very similar to ours, except perhaps for their two weakest expansions, those for CO are systematically larger by about 2 K for  $p_0 d_{\text{eff}} > 10$  mbar-cm. Taking into account the estimated experimental uncertainty of 1 K in this temperature range, the difference might not be

so significant. However, one can also speculate on a slight heating of the jets due to the formation of some clusters in the strongest expansions of Bassi *et al.*,<sup>26</sup> carried out with a ten times smaller nozzle diameter and thus with much larger values of  $p_0 d_{\text{eff}}$ , which is a rough measure of the clustering likelihood.<sup>63</sup> Confidence on the CO and He translational temperatures observed in our experiments for  $p_0 d_{\text{eff}} > 10$  mbar-cm is supported by the remarkable agreement between the  $T_{\parallel, \infty}$  values obtained in our measurements and those computed directly with the CO-He collision cross sections from the literature.<sup>87</sup>

Figure 10 shows the terminal rotational temperatures of CO from 2+2 REMPI measurements reported by Ahern *et al.*<sup>29</sup> for supersonic expansions of pure CO and of very dilute (1%) mixtures of CO in He. The results agree with our measurements within the experimental uncertainty. It is worth noting, that the degree of cooling attained in the CO/He expansions of these authors is comparable to that of our mixture, which is 10 times more concentrated in CO. This supports the previous assumption that in our experiment rotational cooling is also mostly driven by the He thermal bath, whose temperature corresponds approximately to that of an isentropic expansion of a monoatomic gas. Bassi *et al.*<sup>26</sup> measured the terminal populations of CO rotational levels in supersonic beams using diode IR laser excitation and bolometer detection. These authors noted that the rotational populations deviated from a thermal distribution and did not provide rotational temperatures in their work. Nevertheless, approximate values of  $T_{r, \infty}$ , can be obtained by fitting these state populations to a Boltzmann function, and the resulting temperatures are represented in Figure 10. As can be seen, for pure CO expansions these terminal rotational temperatures lie within the experimental uncertainty of our data. In the case of the CO/He mixture, the fit of the rotational populations of Bassi *et al.*<sup>26</sup> leads to rotational temperatures somewhat smaller than those of the present work for  $p_0 d_{\text{eff}} < 10$  mbar cm, whereas for higher  $p_0 d_{\text{eff}}$  values the agreement is good.

Since both Bassi *et al.*<sup>26</sup> and Ahern *et al.*<sup>29</sup> report terminal CO rotational populations, rather than rotational temperatures, a comparison between their measurements and the thermal rotational populations assumed for the approximate simulation of our spectra should be instructive. Such a comparison is shown in Figure 11 for the first three rotational levels of CO in CO-He expansions. The global agreement between the present



results and those from the earlier experiments is remarkably good, although some discrepancies are found in the  $p_{0\text{eff}} \approx 5\text{-}13$  mbar·cm interval, where the  $j=0$  populations determined by the other two groups, especially by the group of Bassi *et al.*,<sup>26</sup> are larger than those corresponding to the present thermal simulations of the spectra and, consequently, give rise to the lower approximate  $T_{r,\infty}$  shown in Figure 10.<sup>89</sup> In expansions of pure CO, the rotational distributions (not shown) determined by Bassi *et al.* and by Arnhem *et al.* deviate less from the Boltzmann shape and are in better agreement with those of the present work.

As far as we know, cross-sections or rate constants for rotational relaxation in CO-Ne collisions below 100 K have not been previously reported. On the other hand, there is a substantial amount of data for low temperature rotational energy transfer processes in CO-CO and CO-He collisions. An extensive comparison of the experimental and theoretical results available for this two latter systems can be found in refs. 32 and 33. Some of these literature cross sections are compared in Figure 12 with those of the present work. We focus first of all on the relaxation cross-sections for pure CO shown in the upper panel of this figure. State-to-state rate constants,  $k_{ij}$ , for rotational energy transfer in CO were determined from the broadening and shifting of Raman lines in the 273-1173 K temperature range by alternatively applying the “modified exponential gap” (MEG)<sup>14</sup> and the “energy corrected sudden” (ECS)<sup>80</sup> fitting laws. Estimates of  $\sigma_{r,\text{CO-CO}}(T)$  down to 20 K, obtained from an extrapolation of these results, were reported by Belikov.<sup>32</sup> As can be seen in Fig. 12, the corresponding cross sections lie in both cases within the estimated uncertainty of our values, although the ECS fitting law provides a closer agreement with our results. Thermal relaxation cross sections at 77 K, obtained in ultrasound absorption experiments<sup>5</sup> and in classical trajectory calculations<sup>56</sup> performed on the *ab initio* PES of van der Pol *et al.*,<sup>45</sup> are also in good agreement with our values. However, a striking discrepancy is found between the EIF results<sup>32</sup> and all the rest. The EIF cross sections grow very fast with decreasing temperature. At 100 K they are roughly three times smaller than ours, but become twice as large at about 20 K. The reason for this contrasting behavior is unclear, especially considering that the systematic discrepancies found between our REMPI detection and the EIF experiments are significantly more marked for CO-CO and for  $\text{N}_2\text{-N}_2$ <sup>73</sup> self collisions than for the CO-He (see below) or  $\text{N}_2\text{-He}$ <sup>70,76</sup> collisions.

The CO-He atom–diatom system is more amenable to rigorous theoretical treatments than its CO-CO diatom-diatom counterpart and accurate quantum close-coupling calculations of state-resolved relaxation rate constants,  $k_{ij}$ , have been reported down to 5 K.<sup>3,83</sup> In particular, the  $k_{ij}$  determined by Green and Thadeus,<sup>83</sup> which include transitions between rotational levels with  $j \leq 6$ , have been the reference values for the Astrophysics community since 1976. More recently, improved rate constants incorporating transitions up to  $j=14$ , were reported by Cecchi-Pestellini *et al.*<sup>3</sup> who used the accurate SAPT PES of Hejmen *et al.*<sup>49</sup> in their calculations. The improved state-to-state rate constants corrected the previous ones by factors within 30% and indicated that the  $k_{ij}$  are influenced at low temperature by shape resonances associated with the attractive van der Waals well.<sup>3,58</sup> Recent experimental rate coefficients for total removal from selected rovibronic states, determined between 294 K and 15 K from spectroscopic measurements performed in a CRESU apparatus,<sup>34</sup> were in very good agreement with those calculated with the  $k_{ij}$  of Cechi-Pestellini *et al.*

The comparison of the above mentioned calculations with the present results requires the evaluation of thermal relaxation cross sections from the theoretical  $k_{ij}$  values. This can be done in a straightforward way by suitably weighting the state resolved rate constants at a given temperature. The following approximate expression has been often used to this aim.<sup>20,33,67,79,90</sup>

$$\sigma_r(T)\langle v \rangle = \sum_{i=0} \sum_{j>i} N_i^* k_{ij} \frac{(E_j - E_i)^2}{\langle E^2 \rangle - \langle E \rangle^2} \quad (10)$$

where  $E_i$  and  $E_j$  are the energies of the  $i$  and  $j$  rotational levels,  $\langle v \rangle$  is the average collision velocity at temperature  $T$ ,  $k_{ij}$  is the rate coefficient for the  $i \rightarrow j$  transition at the same temperature, and  $\langle E^n \rangle = \sum_i N_i^* E_i^n$ , are the moments of the rotational energy

distribution with  $N_i^*$ , the equilibrium population of the  $i$  level, given by:

$$N_i^* = \frac{g_i (2i+1) e^{(-E_i/kT)}}{Q} \quad (11)$$

where  $g_i$  is the nuclear statistical weight of the state (1 in all cases for CO) and  $Q$  the partition function.

The  $\sigma_{r,\text{CO-He}}(T)$  calculated with eq 10 using the close coupling  $k_{ij}$  values of Green and Thadeus<sup>83</sup> and of Cecchi-Pestellini *et al.*<sup>3</sup> are represented in the lower panel of Figure 12 together with the results of the present work. The EIF experimental data of Belikov *et al.*<sup>33</sup> are also included for direct comparison. Note that the calculations with the data from Green and Thadeus are limited to the 5-40 K range because at higher temperatures contributions from  $j>6$ , not available in ref 83, begin to be important according to eq 10. In addition, Fig. 12 also includes, in principle, less accurate theoretical relaxation cross sections obtained from infinite-order sudden (IOS)<sup>33</sup> and classical trajectory calculations<sup>50,54</sup> below  $T=100$  K. As can be observed, between 20 K and 100 K the whole set of experimental and theoretical cross sections, in spite of a certain scatter, lie mostly within the mutual uncertainty and are therefore in reasonable agreement with each other. On the contrary, at temperatures smaller than 20 K, the  $\sigma_{r,\text{CO-He}}(T)$  from our REMPI experiments and that from the EIF measurements diverge gradually. The EIF cross sections grow monotonically with decreasing temperature until  $50 \text{ \AA}^2$  at  $T=6$  K, which is more than two times greater than the values obtained in the present work, where the cross section stabilizes at a value close to  $20 \text{ \AA}^2$  for  $T$  lower than  $\approx 20$  K. The close-coupling (CC) theoretical relaxation cross sections corresponding to the  $k_{ij}$  of Green and Thadeus<sup>83</sup> are closer to the EIF points, while those calculated with the more recent values of Cecchi-Pestellini *et al.*<sup>3</sup> lie somewhere in between. In any case, these theoretical  $\sigma_r(T)$  should be considered with care, since the validity of eq 10 is dubious close to the regime of adiabatic rotation-translation energy transfer,<sup>67,91</sup> which is approached for these very low temperatures.<sup>73</sup> Finally, the exceptionally good overlap observed in Fig. 12 between our values of  $\sigma_{r,\text{CO-He}}(T)$  and those from IOS state-to-state rate constants calculated on the POT0 PES<sup>82</sup> over the whole temperature range 5-100 K is probably fortuitous, since in addition to the use of eq 10, the  $k_{ij}$  from the IOS approximation at low temperatures is expected to be less accurate<sup>79</sup> than the CC calculations.

#### 4. Summary and Conclusions

Translational and rotational relaxation cooling taking place in supersonic expansions of pure CO or CO diluted in Ne or He have been investigated by means of REMPI and TOF techniques. In all cases studied, the final rotational temperatures of CO were found to be higher than the translational temperatures of both mixture components. In the weakest expansions, the terminal translational temperatures of CO were also higher than those of He, indicating a breakdown of the thermal equilibrium between the two coexpanding species in a similar way as found previously in N<sub>2</sub>/He mixtures. By application of a thermal conduction model to describe the energy-momentum exchange in the gas expansion, rotational relaxation cross sections  $\sigma_{r,CO-X}$  (with X=CO, Ne, He) were derived in the  $\approx 5$ -100 K temperature interval. The same model could reproduce well the translational disequilibrium between CO and He by assuming a classical collision cross section (with a  $T^{-\frac{1}{3}}$  dependence) and using literature values for the attractive term of the CO-He interaction.

The temperature dependence of the CO rotational relaxation cross sections follows a similar qualitative trend as previously observed for N<sub>2</sub>. For each collision pair,  $\sigma_{r,CO-X}$  shows initially a monotonic growth as the temperature decreases from 100 K to values of tens of Kelvin. At sufficiently low temperature, however, all the  $\sigma_{r,CO-X}$  cross sections systematically level off, and  $\sigma_{r,CO-CO}$  even shows a maximum at  $T \approx 20$  K. This change of behaviour at low temperature, also found for N<sub>2</sub>, is likely to be associated with the reaching of the adiabatic regime of inefficient rotational-translational transfer as discussed in detail in a previous work.<sup>73</sup> As far as we know, the  $\sigma_{r,CO-Ne}(T)$  reported in this work constitutes the first estimate thus far for the relaxation cross section of the CO-Ne system. A progression  $\sigma_{r,CO-CO} > \sigma_{r,CO-Ne} > \sigma_{r,CO-He}$  is found at the higher temperatures, which changes at  $T < 20$  K to the reverse trend  $\sigma_{r,CO-Ne} > \sigma_{r,CO-CO}$ , thereby indicating that the CO-Ne collisions become more effective for the rotational cooling at sufficiently low temperature. Finally, it is found that  $\sigma_{r,CO-X} > \sigma_{r,N_2-X}$  systematically over the whole temperature range. The implication of this is that the rotational relaxation of the dipolar CO molecule, in both self collisions and in collisions with rare gas atoms, is appreciably more efficient than for the homonuclear N<sub>2</sub> molecule, an aspect that becomes especially noticeable at low temperature  $T < 20$  K.

The present cross sections for relaxation in CO-CO collisions are in good agreement with various literature experimental estimates available below 100 K, but are largely at variance with the values derived from EIF measurements between 100 and 20 K. We are not aware of previous determinations of relaxation cross sections for the CO-CO system at temperatures smaller than 20 K. In the case of CO-He collisions, good accordance is found with available theoretical and experimental data in the 20-100 K temperature interval. Below 20 K the cross sections from this work are smaller than those from EIF measurements. Approximate estimates of the thermal relaxation cross-section, based on accurate state-to-state rate constants lie between ours and the EIF data. Further studies of CO relaxation cross sections at low temperatures, especially state resolved experimental values and accurate theoretical estimates of the cross-sections would be desirable.

### **Acknowledgement**

We thank S. Montero, B. Maté and A. Ramos for their careful reading of the manuscript and for helpful comments. IT thanks the Spanish Ministry of Science and Technology for financial support through the Ramón y Cajal program. JB acknowledges financial support from the EU Research Training Network “Reaction Dynamics” HPRN-CT-1999-00007. GAM and GAP gratefully acknowledge financial support from the Spanish Ministry of Education through the State Secretary of Education and Universities. BMH acknowledges support from the *Plan Andaluz de Investigación* (group FQM-205). Funding by the MEC of Spain under grants FIS2004-00456 and BQU2002-04627-C02-02 and the facilities provided by the Servicio de Espectroscopía Multifotónica (CAI de Espectroscopía) of the Universidad Complutense de Madrid are gratefully acknowledged. This investigation was performed within the framework of the Unidad Asociada “Química-Física Molecular” between the Universidad Complutense and the Instituto de Estructura de la Materia (CSIC).

## Tables

**Table 1.** Attractive terms of the intermolecular potentials ( $C_6$ ) used in eq 8 and fit parameters (F, G) in the expression of the terminal speed ratio (eq 7).

	$\frac{C_6}{k} \times 10^{-43} (\text{K cm}^6)$	F	G
CO	6.18 (ref 87)	1.1	0.31
Ne	0.76 (ref 63)	0.36	0.58
He	0.15 (ref 63)	0.18	0.65

**Table 2:** Best-fit parameters for eq 9 obtained in the present experiments for the rotational relaxation cross sections as a function of temperature of CO in collisions with CO, Ne and He.

	<b>A</b>	<b>B</b>	<b>C</b>	<b>D</b>
<b>CO-CO</b>	17.0	0.35	10	0.20
<b>CO-Ne</b>	6.5	1.60	6	0.20
<b>CO-He</b>	2.5	1.53	6	0.20

## References

- (1) Cernicharo, J. *Astronomy and Astrophysics* **1996**, 315, L201.
- (2) Latter, W. B.; Radford, S. J. E.; Jewell P. R.; Mangum, J. G.; Bally, J. (Eds.) *CO: Twenty-Five Years of Millimeter-Wave Spectroscopy*; Kluwer: Dordrecht 1997.
- (3) Cecchi-Pestellini, C.; Bodo, E.; Balakrishnan, N.; Dalgarno A. *Astrophys J.* **2002**, 571, 1015.
- (4) Kistemaker, P. G., Tom, A., de Vries, A. E. *Physica.* **1970**, 48, 414.
- (5) Prangma, G. J.; Alberga, A. H.; Beenakker, J. J. M. *Physica.* **1973**, 64, 278.
- (6) Trengrove, R. D.; Robjohns, H. L.; Dunlop, P. J. *Ber. Bunsenges. Phys. Chem.* **1984**, 88, 450.
- (7) Haran, E. N.; Maitland, G. C. ; Mustafa, M.; Wakeham, W. A. *Ber. Bunsenges. Phys. Chem.* **1983**, 87, 657.
- (8) Imaishi, N.; Kestin, J.; Wakeman, W. A. *Physica.* **1984**, 123, 50.
- (9) Gianturco, F. A.; Paesani, F.; Laranjeira, M. F.; Vassilenko, V.; Cunha, M. A.; Shashkov, A. G.; Zolotoukhina, A. *Molec. Phys.* **1997**, 92, 957.
- (10) Bouanich, J. P. *J. Quant. Spectrosc. Radiat. Transfer.* **1972**, 12, 1399.
- (11) Nerf, Jr. R. B.; Sonnenberg, M. A. *J. Mol. Spectrosc.* **1975**, 58, 474.
- (12) Belbruno J. J. ; Gelfand, J. ; Radigan, W. ; Verges, K. *J. Molec. Spectrosc.* **1982**, 94, 336.
- (13) Willey, D. R.; Crownover, R. L.; Bittner, D. N.; De Lucia, F. C. *J. Chem. Phys.* **1988**, 89, 1923.
- (14) Rosasco, G. J.; Rahn, L. A.; Hurst, L. A.; Palmer, R. E.; Dohne, S. M. *J. Chem. Phys.* **1989**, 90, 4059.
- (15) Looney, J. P.; Rosaoco, G. J.; Rahn, L. A.; Hurst, W. S.; Hahn, J. W. *Chem. Phys. Lett.* **1989**, 161, 232..
- (16) Doce, J.; Mader, H.; Shwarz, R.; Guarnieri, A. *Molec. Phys.* **1994**, 81, 547.
- (17) Beakey, M. M., Goyette, T. M. ; De Lucia, F. C. *J. Chem. Phys.* **1996**, 105, 3994.
- (18) Boissoles, J.; Thibault, F.; Domenech, J.L.; Bermejo, D.; Boulet, C.; Hartmann, M. *Chem. Phys.* **2001**, 115, 7420.
- (19) Thibault, F.; Martinez, R. Z.; Domenech, J. L.; Bermejo, D.; Bouanich, J. P. *Chem. Phys.* **2002**, 117, 2523.
- (20) Martinez, R. Z.; Domenech, J. L.; Bermejo, D.; Thibault, F.; Bouanich, J. P.; Boulet, C. *J. Chem. Phys.* **2003**, 119, 10563.
- (21) Phipps, S. P.; Smith, T. C.; Hager, G. D.; Heaven, M. C.; McIver, J. K.; Rudolph, W. G. *J. Chem. Phys.* **2002**, 116, 9281.
- (22) Hostutler, D. A.; Smith, T. C.; Hager, G. D.; McBane, G. C.; Heaven, M. C. *J. Chem. Phys.* **2004**, 120, 7483.
- (23) Smith, T. C.; Hostutler, D. A.; Hager, G. D.; Heaven, M. C.; McBane, G. C. *J. Chem. Phys.* **2004**, 120, 2285.
- (24) Keil, M.; Slankas, J. T.; Kuppermann, A. *J. Chem. Phys.* **1979**, 70, 541.
- (25) Faubel, M.; Kohl, K.; Toennies, J. P. *J. Chem. Phys.* **1980**, 73, 2506.
- (26) Bassi, D.; Boschetti, A.; Marchetti, S.; Scoles, G.; Zen, M. *J. Chem. Phys.* **1981**, 74, 2221.
- (27) Belikov, A. E.; Smith M. A. *J. Chem. Phys.* **1999**, 10, 8513.

- (28) Belikov, A. E. ; Strekalov, M. L. ; Storozhev, A. V. *Chem. Phys. Lett.* **1999**, *304*, 253.
- (29) Ahern, M. M.; Steinhurst, D. A.; Smith, M. A.; *Chem. Phys. Lett.* **1999**, *300*, 681.
- (30) Antonova, S.; Lin, A.; Tsakotellis, A. P.; McBane, G. C. *J. Chem. Phys.* **1999**, *110*, 11742.
- (31) Antonova, S.; Lin, A.; Tsakotellis, A. P.; McBane, G. C. *J. Chem. Phys.* **1999**, *110*, 2384.
- (32) Belikov, A. E. *Mol. Phys.* **2000**, *98*, 343.
- (33) Belikov, A. E.; Storozhev, A.V.; Strekalov, M. L.; Smith, M. A. *Mol. Phys.* **2001**, *99*, 559.
- (34) Carty, D.; Goddard, A. Sims, I. R.; Smith, I. W. M. *J. Chem. Phys.* **2004**, *121*, 4671.
- (35) Randall, R. W.; Cliffe, A. J.; Howard, B. J. McKellar, A. R. W. *Mol. Phys.* **1993**, *79*, 1113.
- (36) Chuaqui, C. E.; Le Roy, R. J.; McKellar, A. R. W. *J. Chem. Phys.* **1994**, *101*, 39.
- (37) Havenith, M.; Petri, M.; Lubina, C.; Hilpert, G.; Urban, W. *J. Molec. Spectrosc.* **1994**, *167*, 248
- (38) Chan, M. C.; McKellar, A. R. W. *J. Chem. Phys.* **1997**, *105*, 7910.
- (39) Walker, K. A.; Ogata, T.; Jäger, W.; Greey, M. C. L.; Ozier, I. *J. Chem. Phys.* **1997**, *106*, 7519.
- (40) McKellar, A. R. W.; Can, M. C. *Mol. Phys.* **1998**, *93*, 253.
- (41) McKellar, A. R. W.; Xu, Y.; Jaeger, W.; Bissonette, C. *J. Chem. Phys.* **1999**, *110*, 10766.
- (42) Roth, D. A.; Surin, L. A. ; Dumesh B. S.; Winnewiser, G.; Pak, I. *J. Chem. Phys.* **2000**, *113*, 3034.
- (43) McKellar, A. R. W. *J. Chem. Phys.* **2001**, *115*, 3571.
- (44) Tang, J. McKellar, A. R. W.; Surin, L. A.; Fourizkov, D. N.; Dumesh, B. S. Winnewisser, G. *J. Molec. Spectrosc.* **2002**, *214*, 87.
- (45) van der Pol, A.; van der Avoird, A.; Wormer, P. E. S. *J. Chem. Phys.* **1990**, *92*, 7498.
- (46) Le Roy, R. J.; Bissonnette, C.; Wu, T. H.; Dahm, A. K.; Meath, W. J. *Faraday Discuss. Chem. Soc.* **1994**, *97*, 81.
- (47) Moszynski, R.; Korona, T.; Wormer, P. E. S.; van der Avoird, A. *J. Chem. Phys.* **1995**, *103*, 321.
- (48) Moszynski, R.; Korona, T.; Wormer, P.E.S.; van der Avoird, A. *J. Phys. Chem. A* **1997**, *101*, 4690.
- (49) Heijmen, T. G. A.; Moszynski, R.; Wormer, P.E.S.; van der Avoird A. *J. Chem. Phys.* **1997**, *107*, 9921.
- (50) Gianturco, F. A.; Paesani, F.; Laranjeira, M. F.; Vassilenko, V.; Cunha, M. A.; Shashkov, A. G.; Zolotoukhina, A. *Molec. Phys.* **1998**, *94*, 605.
- (51) McBane, G. C.; Cybulski, S. M. *J. Chem. Phys.* **1999**, *110*, 11734.
- (52) Subramanian, V.; Chitra, K.; Sivanesan, D.; Amutha, R.; Sankar, S. *Chem. Phys. Lett.* **1999**, *307*, 493.
- (53) Tockzylowski, R. R.; Cybulski, S. M. *J. Chem. Phys.* **2000**, *112*, 4604.



- (54) McCourt, F. R. W.; Ter Horst, M. A.; Heck, E. L.; Dickinson, S. A. *Mol. Phys.* **2002**, *100*, 3893.
- (55) Vissers, G. W. M.; Wormer, P. E. S.; van der Avoird A. *Phys. Chem. Chem. Phys.* **2003**, *5*, 4767.
- (56) Heck, E. L.; Dickinson A. S. *Physica A*. **1995**, *217*, 107.
- (57) Bodo, E.; Gianturco, F. A.; Paesani, F. Z. *Phys. Chem. Int.* **2000**, *214*, 1013.
- (58) Balakrishnan, N.; Dalgarno, A.; Forrey, R. C.; *J. Chem. Phys.* **2000**, *113*, 621.
- (59) Pirumov, U. G.; Roslyakov, G. S. *Gas Flow in Nozzles*; Springer Verlag: Berlin, Heidelberg, **1986**.
- (60) Tejada, G.; Maté, B.; Fernández-Sánchez, J. M.; Montero, S. *Phys. Rev. Lett.* **1996**, *76*, 34.
- (61) Maté, B.; Tejada, G.; Montero, S. *J. Chem. Phys.* **1998**, *108*, 2676.
- (62) Maté B.; Gaur, I. A.; Elizarova, T.; Chirokov, I.; Tejada, G.; Fernández, J. M.; Montero, S. *J. Fluid Mech.* **2001**, *426*, 177.
- (63) Miller, D. R. In *Atomic and Molecular Beam Methods (vol 1)*; Scoles, G., Ed.; Oxford University Press: New York 1988.
- (64) Abad, L.; Bermejo, D.; Herrero, V. J.; Santos, J.; Tanarro, I. *J. Phys. Chem. A* **1997**, *101*, 9276.
- (65) Rowe, B. R.; Dupeyrat, G.; Marquette, J. B.; Gaucherel, P. *J. Chem. Phys.* **1984**, *80*, 4195.
- (66) James, P. L.; Sims, J. R.; Smith, I. W. H.; Alexander, M. h.; Yang, M. B. *J. Chem. Phys.* **1998**, *109*, 3882.
- (67) Belikov, A. E. ; Burshtein, A. I. ; Dolgushev, S. V. ; Storozhev, A. V. ; Strekalov, M. L. ; Sukhinin, G. I. ; Sharafutdinov, R. G. *Chem. Phys.* **1989**, *139*, 239.
- (68) Belikov, A. E. ; Sharafutdinov, R. G., Strekalov. M. L. *Chem. Phys. Lett.* **1994**, *231*, 444.
- (69) Belikov, A. E. ; Sharafutdinov, R. G. *Chem. Phys. Lett.* **1995**, *241*, 209.
- (70) Belikov, A. E. ; Sharafutdinov, R. G. ; Storozhev, A. V. *Chem. Phys.* **1996**, *213*, 319.
- (71) Faubel, M.; Weiner, R. E. *J. Chem. Phys.* **1981**, *75*, 641.
- (72) Campargue, R.; Gaveau, M. A.; Lebéhot, A. *Rarefied Gas Dynamics 14<sup>th</sup> Symposium*; Oguchi H. Ed.; University of Tokyo Press: Tokio, 1984. Vol II, p.551.
- (73) Aoiz, F. J.; Diez-Rojo, T.; Herrero, V. J.; Martínez-Haya, B.; Menéndez, M.; Quintana, P., Ramonat, L.; Tanarro, I., Verdasco, E. *J. Phys. Chem. A* **1999**, *103*, 823.
- (74) Aoiz, F. J.; Bañares, L.; Herrero, V. J.; Martínez-Haya, B.; Menéndez, M.; Quintana, P.; Tanarro, I.; Verdasco, E. *J. Phys. Chem. A* **2001**, *105*, 6976.
- (75) Aoiz, F. J.; Bañares, L., Herrero, V. J., Martínez-Haya, B.; Menéndez, M., Quintana, P.; Tanarro, I.; Verdasco, E. *Vacuum* **2002**, *64*, 417.
- (76) Aoiz, F. J.; Bañares, L.; Herrero, V. J.; Martínez-Haya, B.; Menéndez, M.; Quintana, P.; Tanarro, I.; Verdasco, E. *Chem. Phys. Lett.* **2003**, *367*, 500.
- (77) Ramos, A. *Ph. D. Thesis*, Universidad Complutense, Madrid, 2001.
- (78) Ramos, A.; Tejada, G.; Fernández, J. M.; Montero, S. *Phys. Rev. A* **2002**, *66*, 022702.

- (79) Maté, B.; Thibault, F.; Ramos, A.; Tejada, G.; Fernández, J. M.; Montero, S. *J. Chem. Phys.* **2003**, *118*, 4477.
- (80) Sharafutdinov, R. G.; Belikov, A. E.; Strekalov, M. L.; Storozhev, A. V. *Chem. Phys.* **1996**, *207*, 193.
- (81) Heck, E. L.; Dickinson, A. S. *Mol. Phys.* **1997**, *91*, 31.
- (82) Gianturco, F. A.; Sanna, N.; Serna-Molinera, S. *Molec. Phys.* **1994**, *81*, 421.
- (83) Geen, S.; Thaddeus, P.; *Astrophys. J.* **1976**, *205*, 766.
- (84) Abad, L.; Bermejo, D.; Herrero, V. J.; Santos, J.; Tanarro, I. *Rev. Sci. Instrum.* **1995**, *66*, 3826.
- (85) Huber, K. P.; Herzberg, G. *Molecular Spectra and Molecular Structure. Constants of Diatomic Molecules*, Van Nostrand Reinhold 1979.
- (86) Beijerinck H. C. W.; Verster, N. F. *Physica* **1981**, *111C*, 327.
- (87) Rijks W.; Wormer, P. E. S. *J. Chem. Phys.* **1989**, *90*, 6507.
- (88) Aoiz, F. J.; Verdasco, J. E.; Herrero, V. J.; Sáez Rábanos V.; Alexander, M. J. *Chem. Phys.* **2003**, *119*, 5860.
- (89) Note that in Figure 8 of ref 33 there is an apparent discrepancy between the rotational populations of Bassi *et al.*<sup>26</sup> and those of Ahern *et al.*<sup>29</sup>. This is due to the fact that in that figure, instead of the relative populations,  $N_j$ , of Bassi *et al.*, the degeneracy corrected values,  $N'_j = N_j/2(j+1)$  with the normalization  $\sum_j N'_j = 1$  have been represented. Once the actual  $N_j$  values are taken, good agreement is found.
- (90) Sukhinin, G. I. *Zh. Prikl. Mech. Tekn. Fiz.* **1988**, *1*, 31 (*J. Appl. Mech. Tech. Phys.* **1988**, *30*, 1).
- (91) Strekalov, M. L. *Khim. Fiz.* **1988**, *7*, 1182.

## Figure Legends

**Figure 1.** (a) 2+2 REMPI spectrum of the  $A^1\Pi(v=3) \leftarrow X^1\Sigma^+(v=0)$  transition in CO recorded in a molecular beam corresponding to an expansion with  $p_0d_{\text{eff}}=85$  mbar cm. (b) Same as (a) but using a 2+1' REMPI scheme. (c) Simulation of the spectrum with a rotational temperature of 3 K.

**Figure 2.** Experimental (top) and simulated (bottom) 2+1' REMPI spectrum of the  $A^1\Pi(v=3) \leftarrow X^1\Sigma^+(v=0)$  transition from an effusive beam of pure CO at 298 K.

**Figure 3.** Typical molecular beam REMPI spectra (top of each panel) corresponding to different expansions of pure CO together with their simulations (bottom of each panel) with indication of the corresponding rotational temperatures,  $T_{r,\infty}$ .

**Figure 4.** Molecular beam time-of-arrival distributions for three different expansions of pure CO at similar values of  $p_0d_{\text{eff}}$  as those of Figure 3. The points represent the experimental data and the lines the corresponding simulations. The terminal flow velocities,  $u_\infty$ , and parallel translational temperatures,  $T_{||,\infty}$ , derived from the simulations are also indicated.

**Figure 5.** Terminal flow velocities (top) and temperatures (bottom) in expansions of pure CO. (Upper panel) Symbols: experimental data. Line: model calculations using eq 5. (Lower panel) Closed circles: experimental terminal translational temperatures. Dashed line: model calculation with eq 6. Open triangles: experimental terminal rotational temperatures. Solid line: result of the integration of eq 4 with the  $\sigma_{r,\text{CO-CO}}$  of Figure 8.

**Figure 6.** Terminal flow velocities (top) and temperatures (bottom) in expansions of CO(10%)+Ne. (Upper panel) Solid circles: experimental data for CO. Open circles: experimental data for Ne. Line: model calculations using eq 5. (Lower panel) Closed circles: experimental terminal translational temperatures for CO. Open circles: same for Ne. Dashed line: model calculation with eq 6. Open triangles: experimental terminal

rotational temperatures. Solid line: result of the integration of eq 3 with the  $\sigma_{r,CO-Ne}$  of Figure 8.

**Figure 7.** Terminal flow velocities (top) and temperatures (bottom) in expansions of CO(12%)+He. (Upper panel) Solid circles: experimental data for CO. Open circles: experimental data for He. Line: model calculations using eq 5. (Lower panel) Closed circles: experimental terminal translational temperatures for CO. Open circles: same for He. Open triangles: experimental terminal rotational temperatures. Dashed line: model calculation with eq 6. Dotted and solid lines: results of the integration of eq 1 for  $T_{t,CO}$  and  $T_{r,CO}$  using the  $\sigma_{r,CO-CO}$  of Figure 8 and  $\sigma_{c,CO-He} = (56 C_{6,CO-He} / kT)^{\frac{1}{3}}$  with  $C_{6,CO-He}$  taken from ref 87.

**Figure 8.** Thermal cross sections for rotational relaxation,  $\sigma_r(T)$ , in CO-CO, CO-Ne and CO-He (solid lines) derived from the measurements of the present work and comparison with the corresponding cross sections for  $N_2-N_2$ <sup>73</sup>,  $N_2-Ne$ <sup>74</sup> and  $N_2-He$ <sup>76</sup> (dashed lines), measured with the same technique.

**Figure 9.** Comparison of final translational temperatures in expansions of pure CO (upper panel) and of CO/He mixtures (lower panel). (Upper panel) Solid circles: data from ref 26. Open circles: data from the present work. Dashed line: same as in Figure 5. (Lower panel) Solid triangles and solid circles: final translational temperatures reported in ref 26 for He atoms and CO molecules, respectively, expanded from a CO(10%)+He mixture. Open triangles and open circles: final translational temperatures measured in this work for He atoms and CO molecules, respectively, expanded from a CO(12%)+He mixture. Dashed and dot lines: same as in Figure 7.

**Figure 10.** Comparison of final rotational temperatures in expansions of pure CO (upper panel) and of CO/He mixtures (lower panel). (Upper panel) Solid circles: present data. Open circles: data from the fit of the IR rotational populations of ref 26 to a Boltzmann distribution. Open triangles: temperatures from the REMPI measurements of ref 29. Solid line: same as in Figure 5. Lower panel. Solid circles: present data. Open circles: temperatures derived from a fit of the IR rotational populations of ref 26 to a Boltzmann distribution. Open triangles: temperatures from the REMPI measurements of ref 29 corresponding to a CO(1%)+He mixture.

**Figure 11.** Relative terminal populations of the three first rotational levels of CO in the same supersonic expansions of CO/He mixtures of Figure 10. Solid circles: populations corresponding to the rotational temperatures used to simulate the experimental spectra of the present work. Open circles: rotational populations derived from the IR measurements of ref 26. Open triangles: rotational populations from the REMPI measurements of ref 29.

**Figure 12.** Comparison of available thermal relaxation cross sections for CO-CO (upper panel) and CO-He (lower panel) collisions. (Upper panel) Solid line: present results. Open circles: EIF values from ref 32. Dashed line: estimate reported in ref 32 from the application of the ECS fitting law to line broadening data<sup>80</sup>. Dotted line: estimate reported in ref 32 from the application of the MEG fitting law to line broadening data<sup>14</sup>. Inverted triangle: from the ultrasound absorption experiments of ref 5. Black square: from the classical trajectory calculations of ref 56. Lower panel. Solid line: present results. Open circles: from the EIF measurements of ref 33. Dotted line: calculated with eq 10 using the CC state-to-state rate coefficients of ref 83. Dashed line: calculated with eq 10 using the CC state-to-state rate coefficients of ref 3. Dash-dot-dot line: IOS calculation<sup>33</sup> on POT0 PES<sup>82</sup>. Dash-dot line: classical trajectory calculations from ref 50. Black square: Classical trajectory calculation from ref 54.

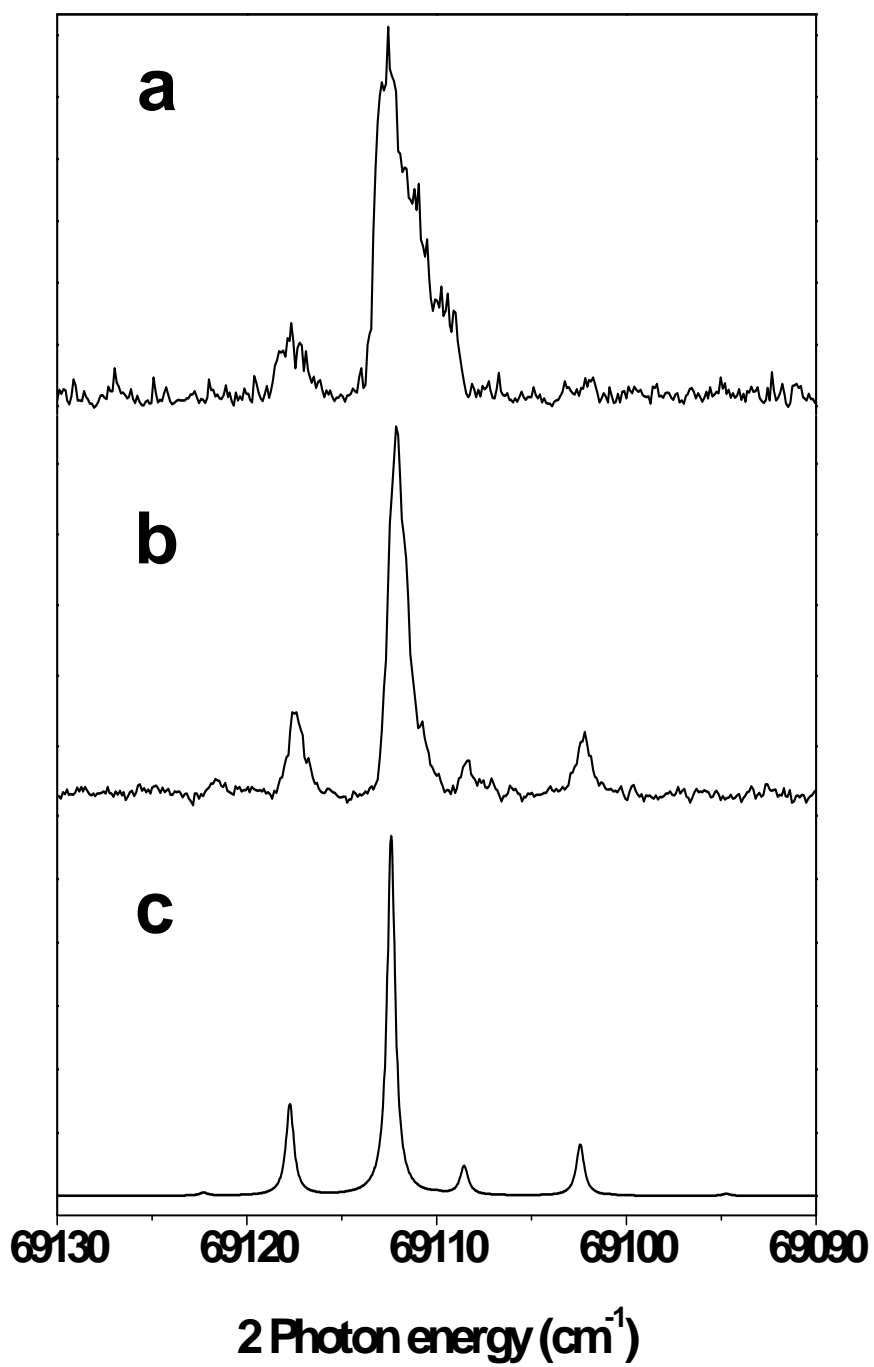


Figure 1 Amaral et al.

CO  $A^1\Pi, v=3 \leftarrow X^1\Sigma^+, v=0$

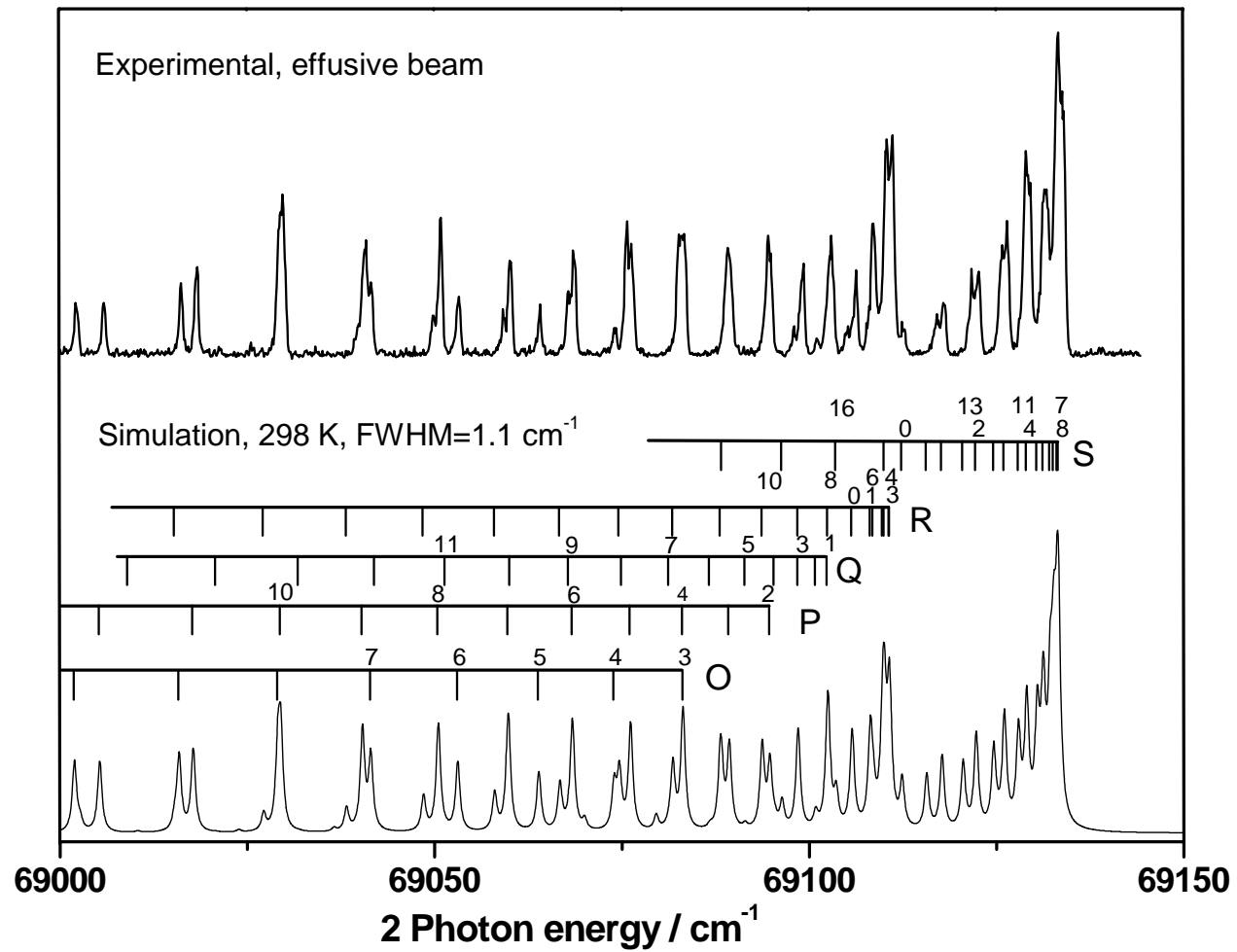


Figure 2 Amaral et al.

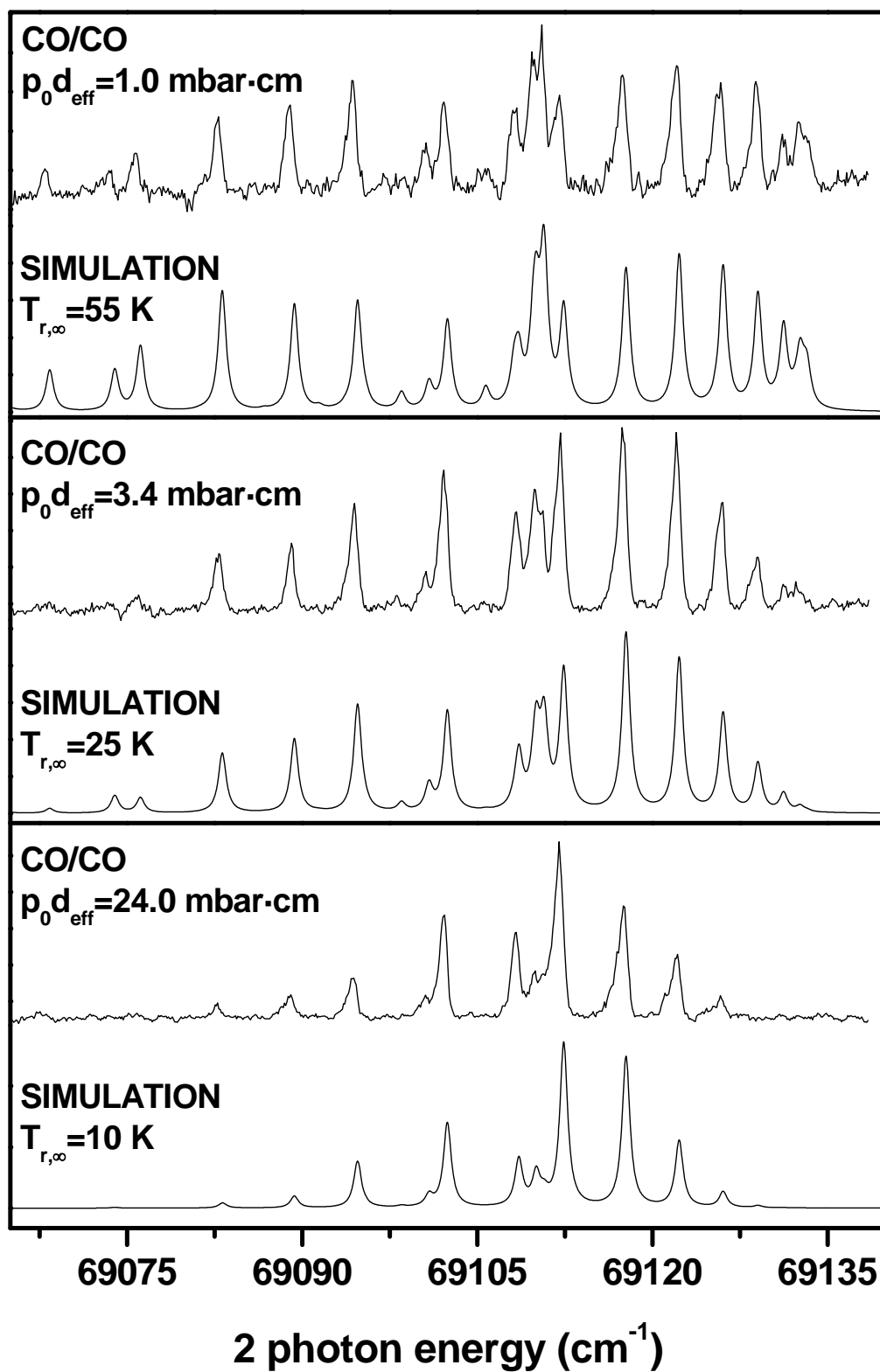


Figure 3 Amaral et al.



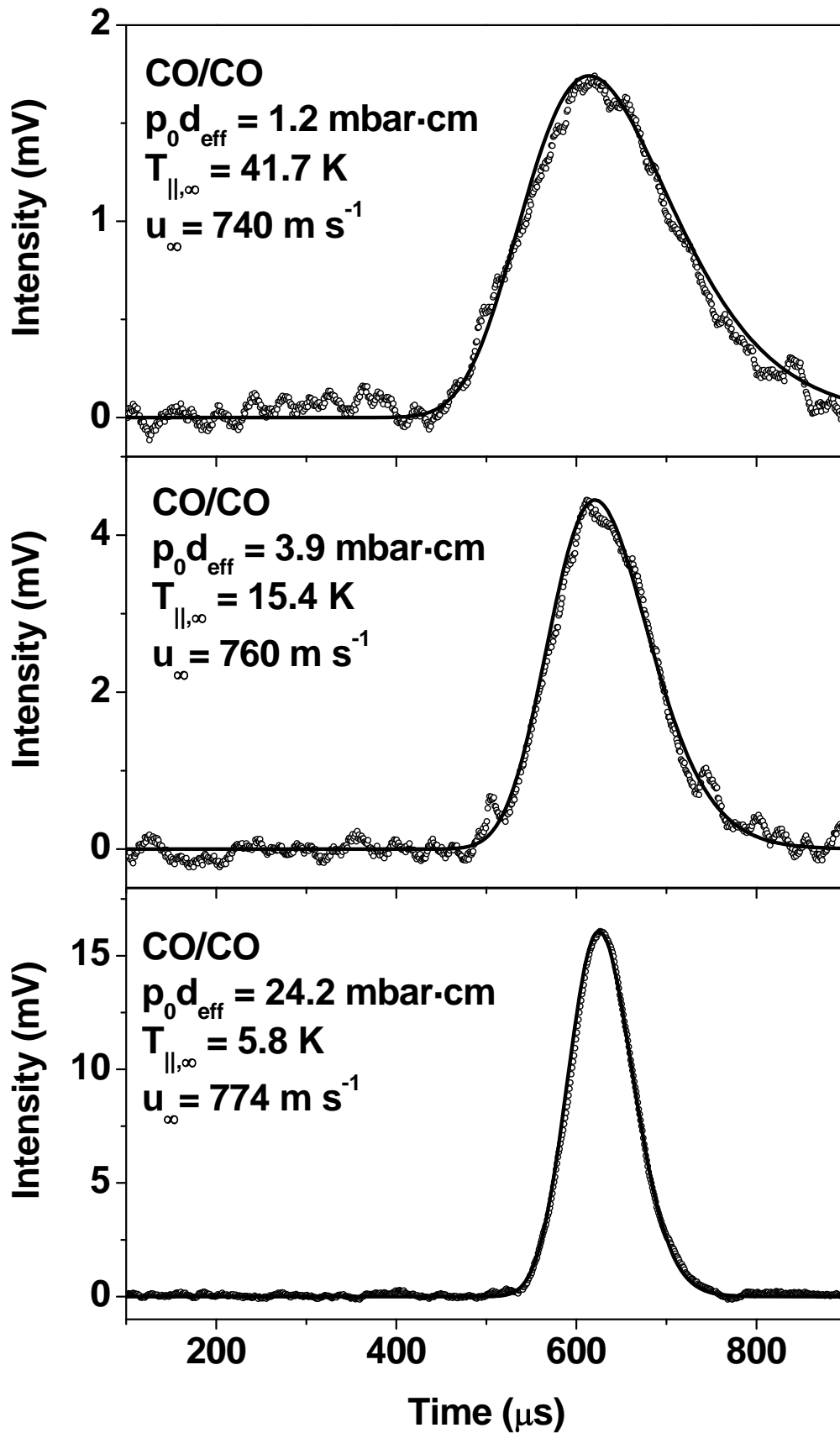


Figure 4 Amaral et al.

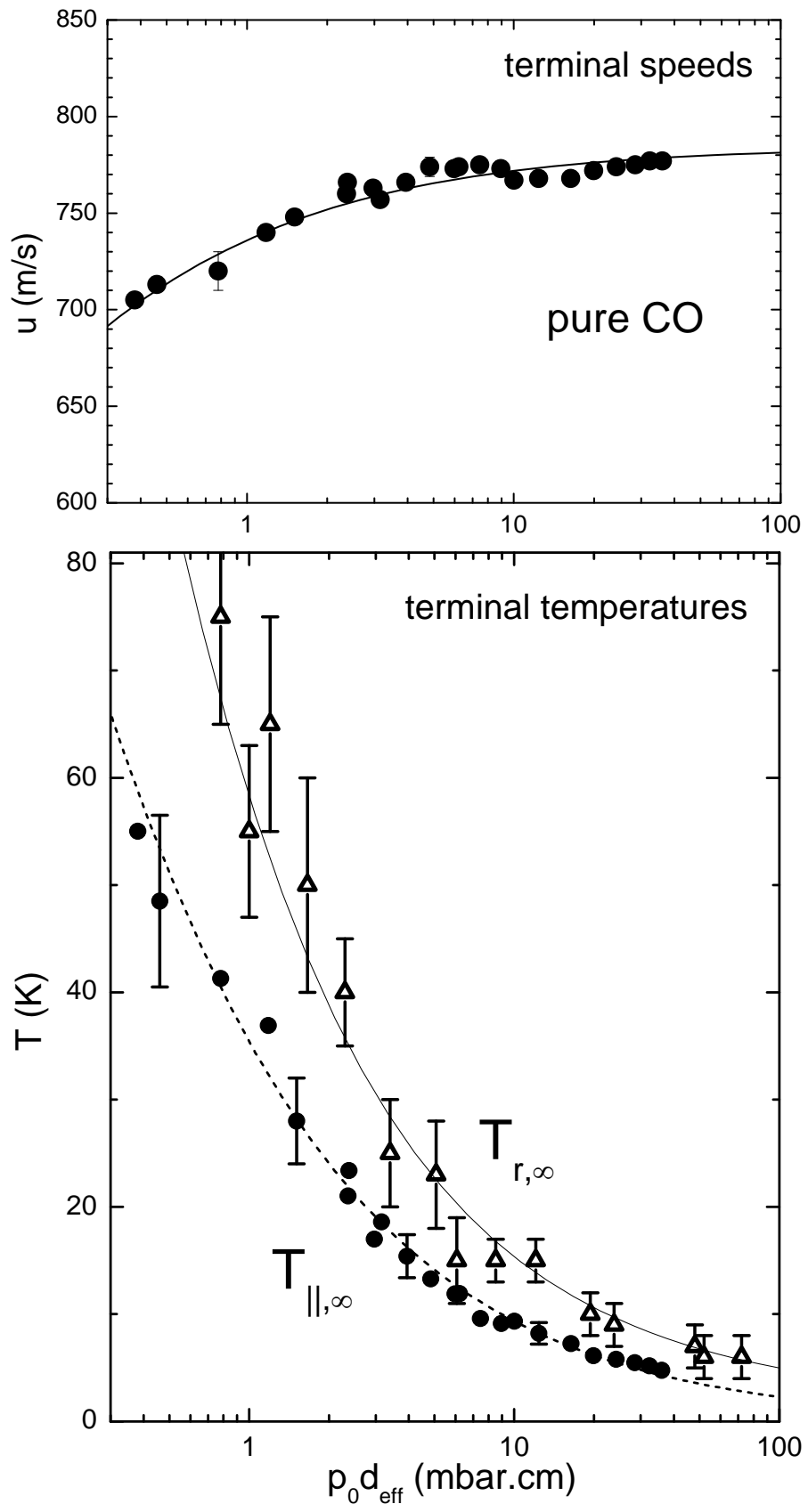


Figure 5 Amaral et al.

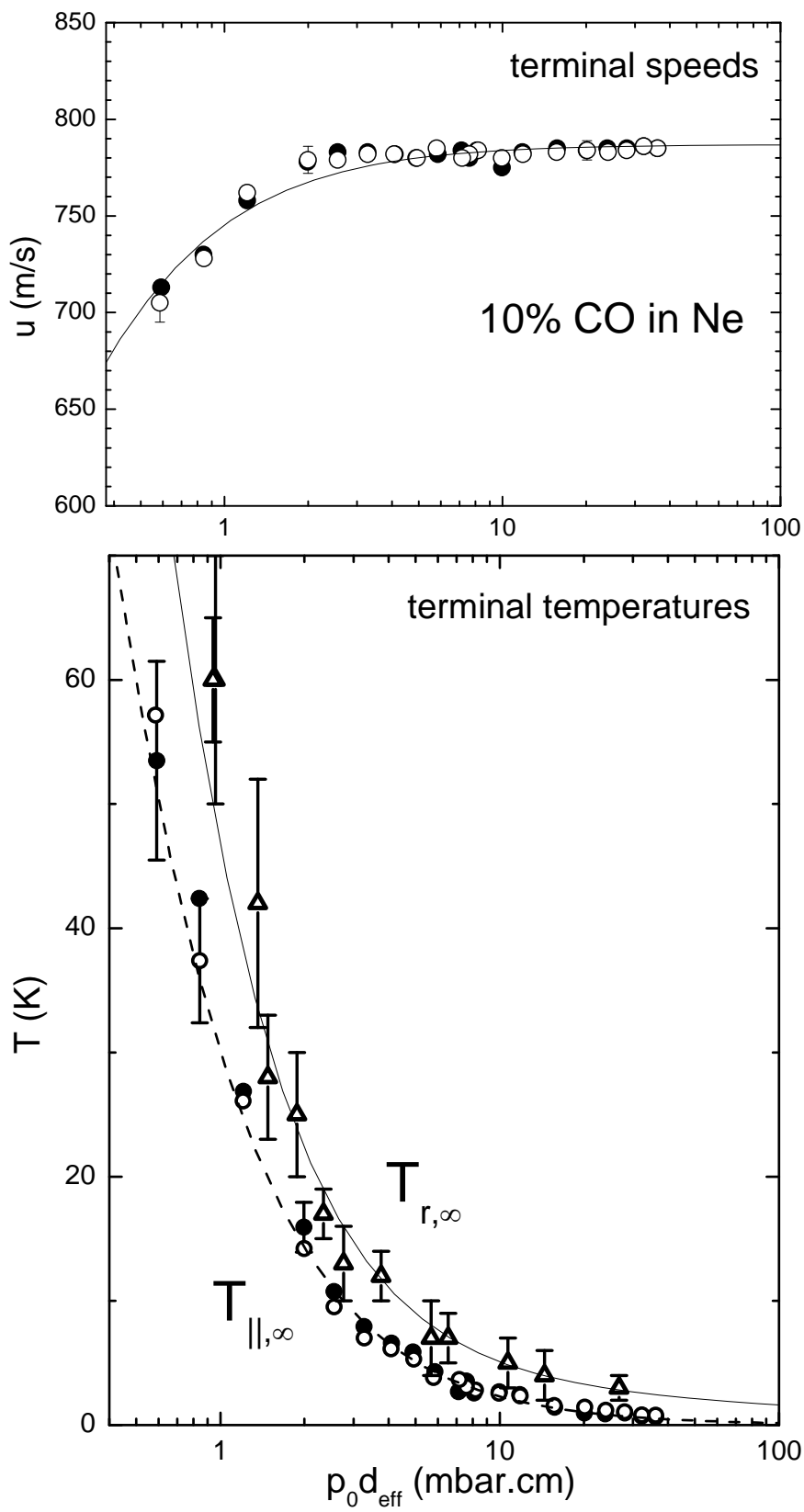


Figure 6 Amaral et al.

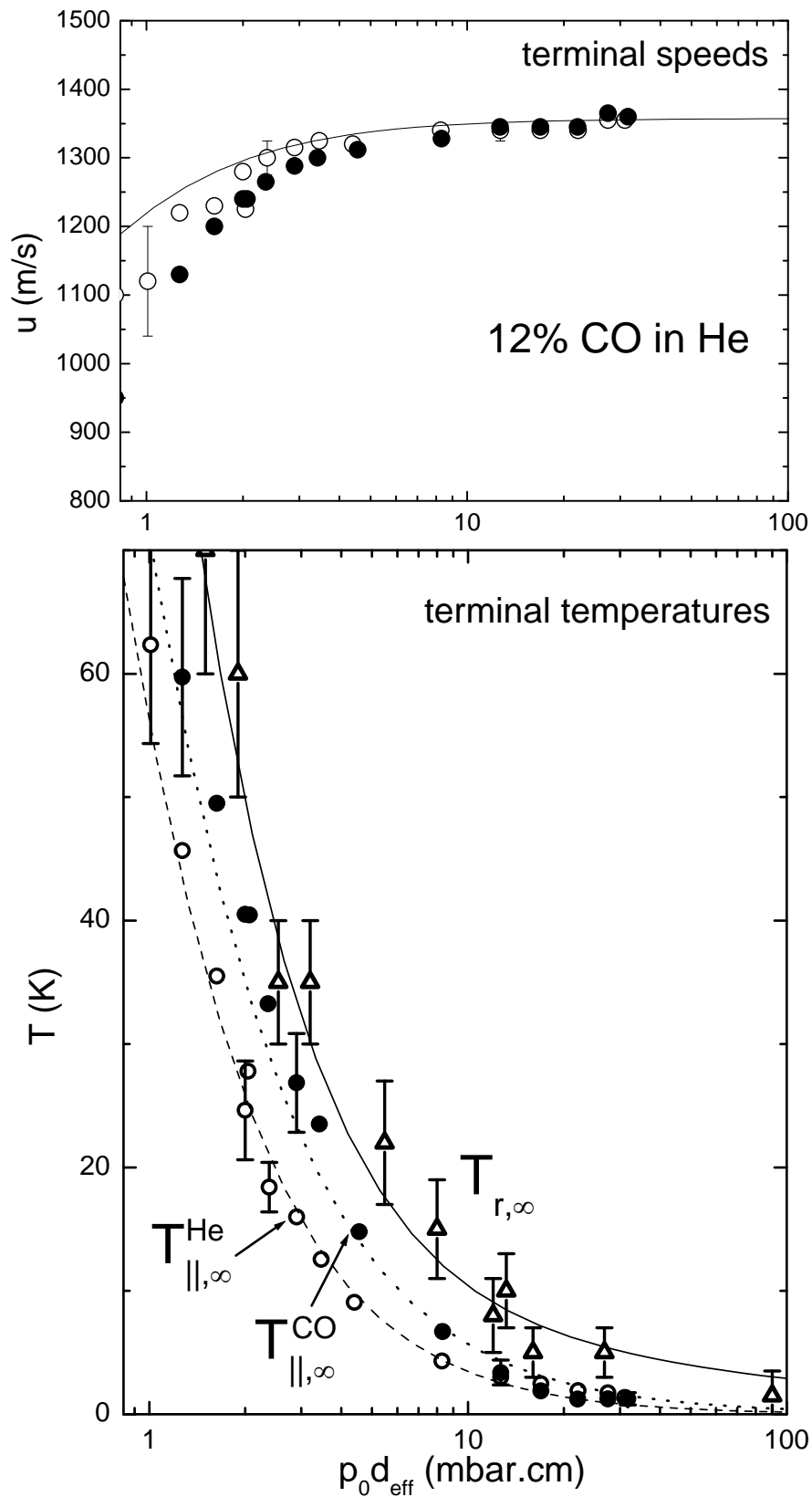


Figure 7 Amaral et al.

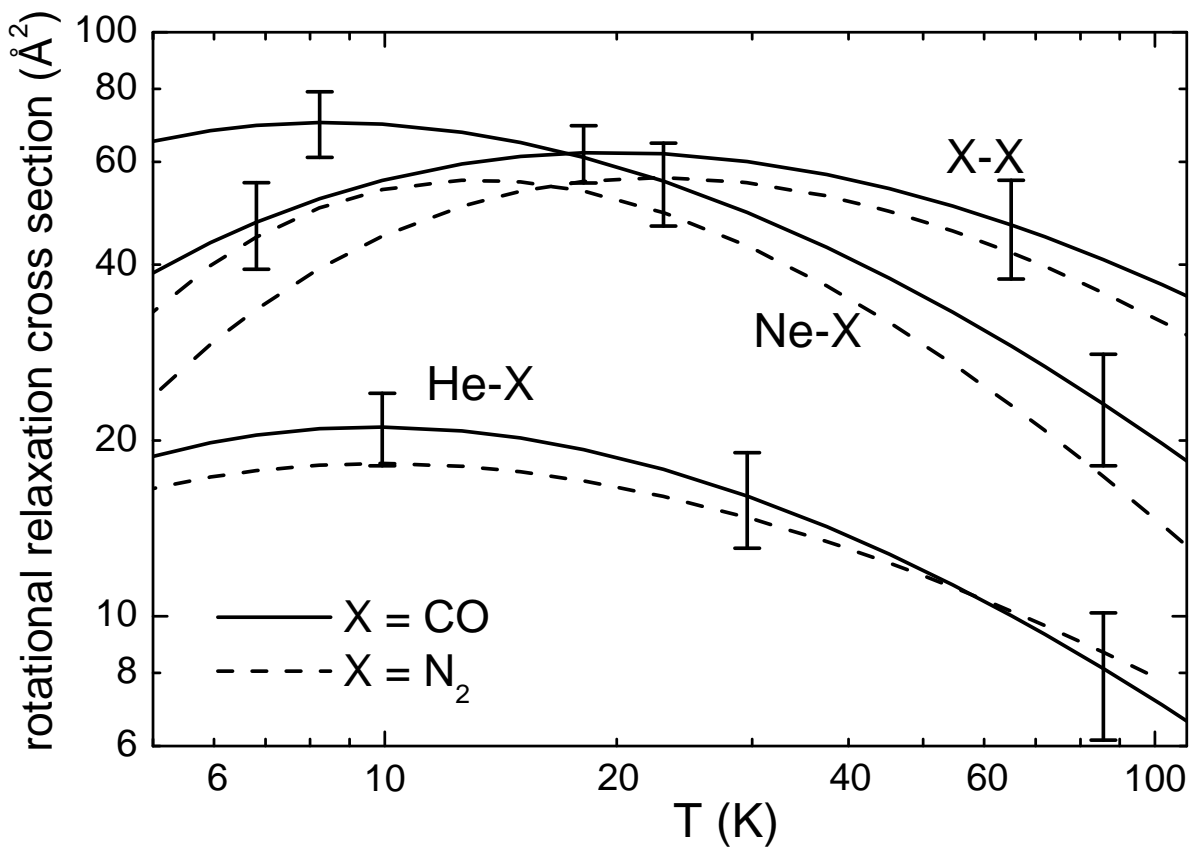


Figure 8 Amaral et al.

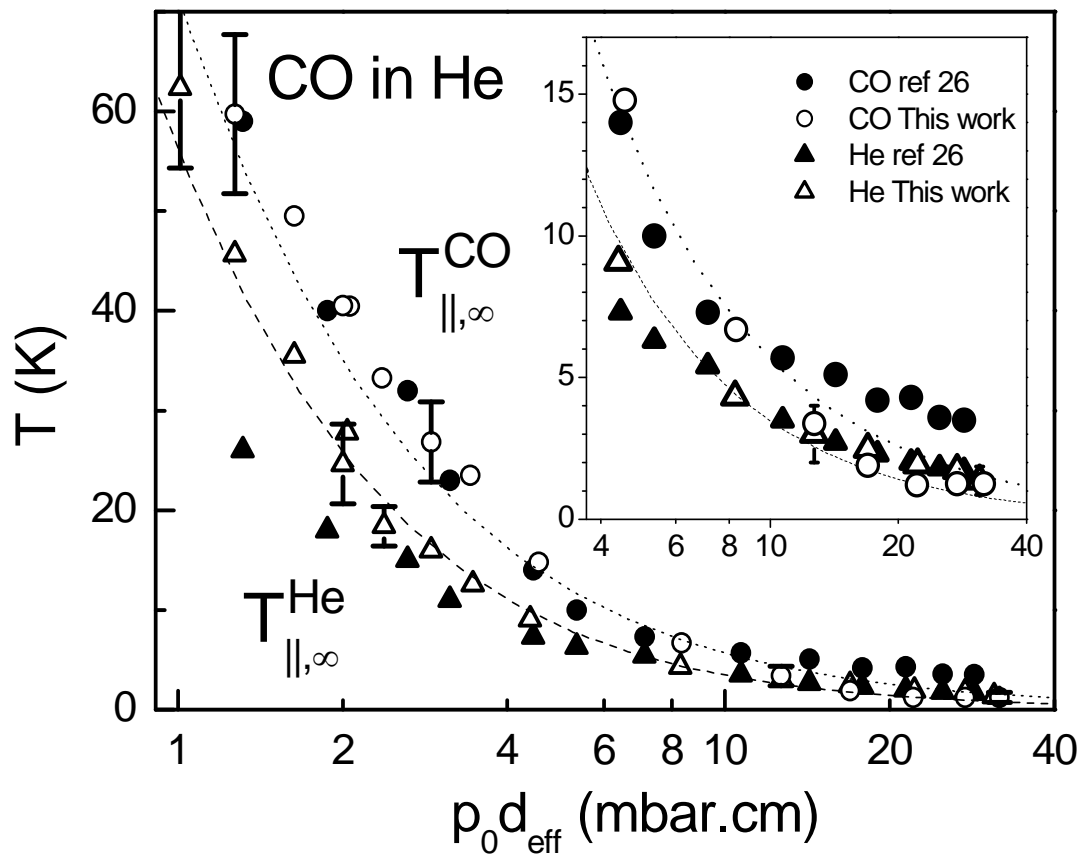
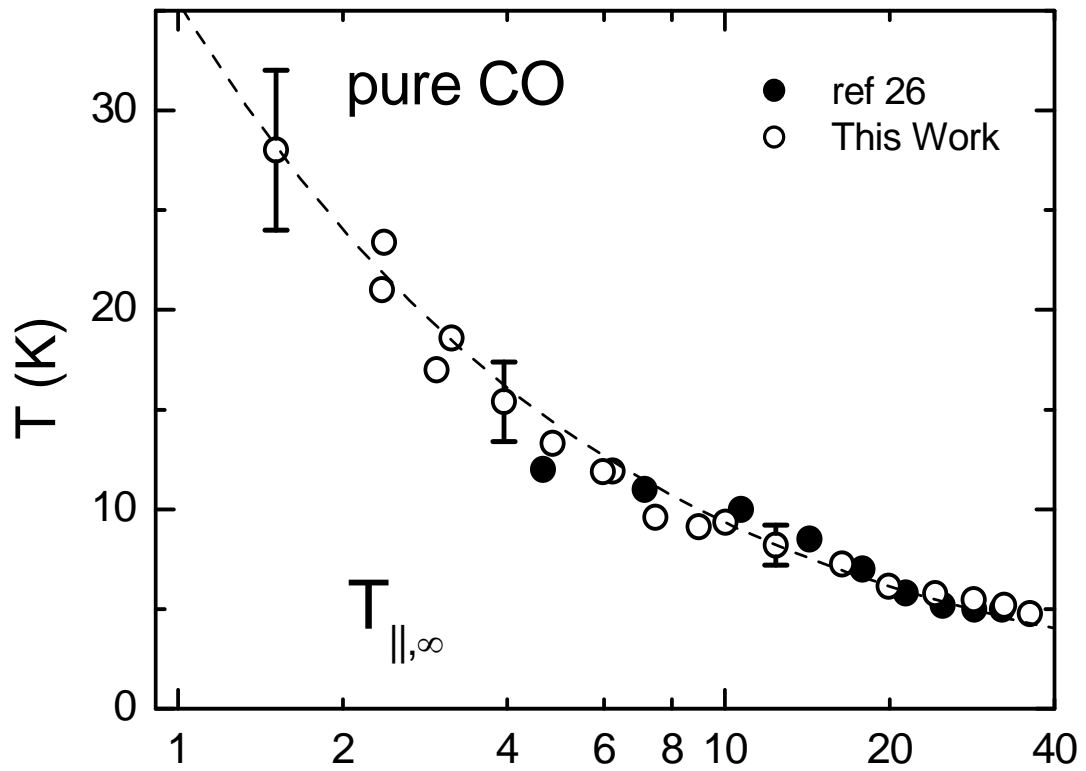


Figure 9 Amaral et al.

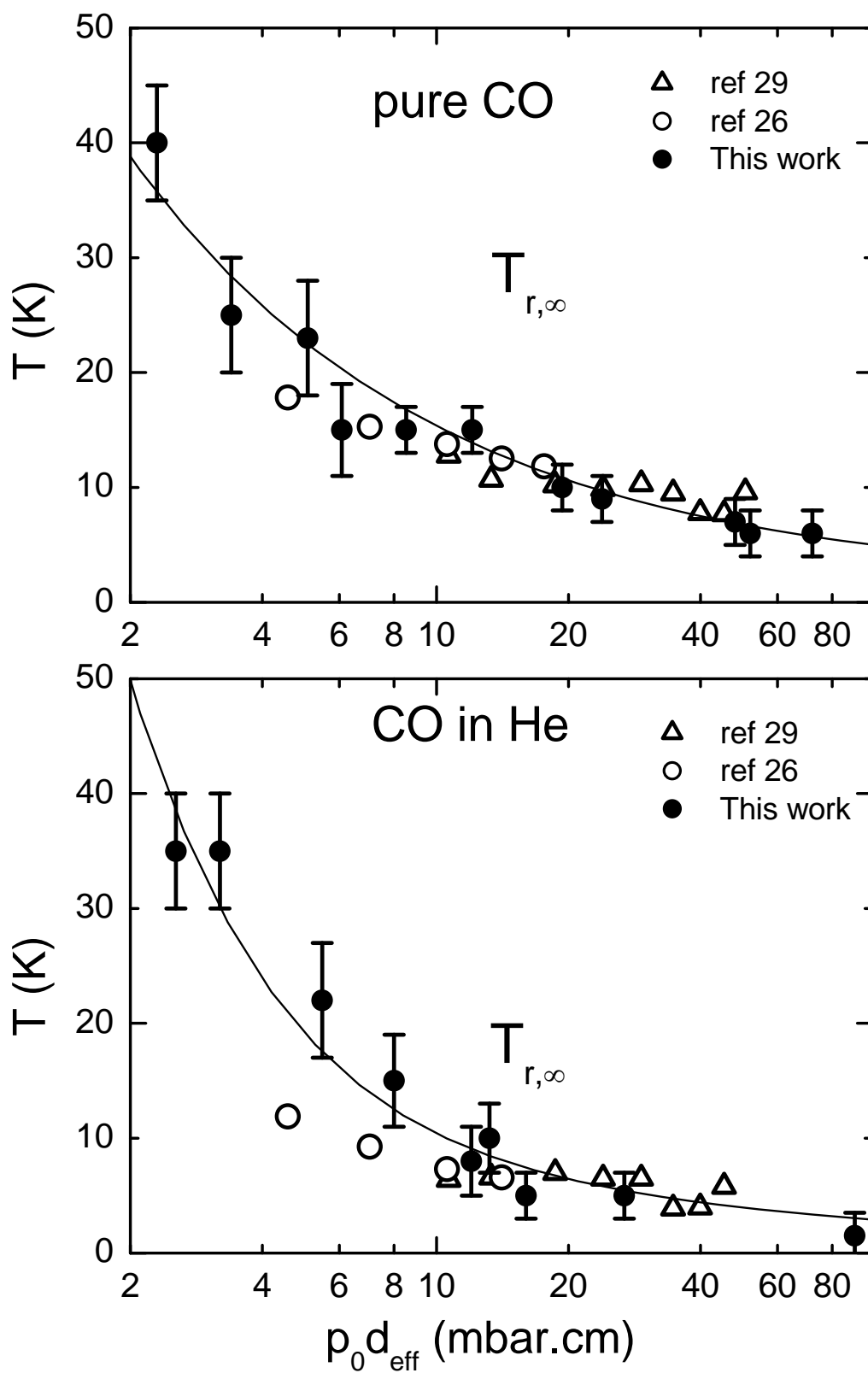


Figure 10 Amaral et al.

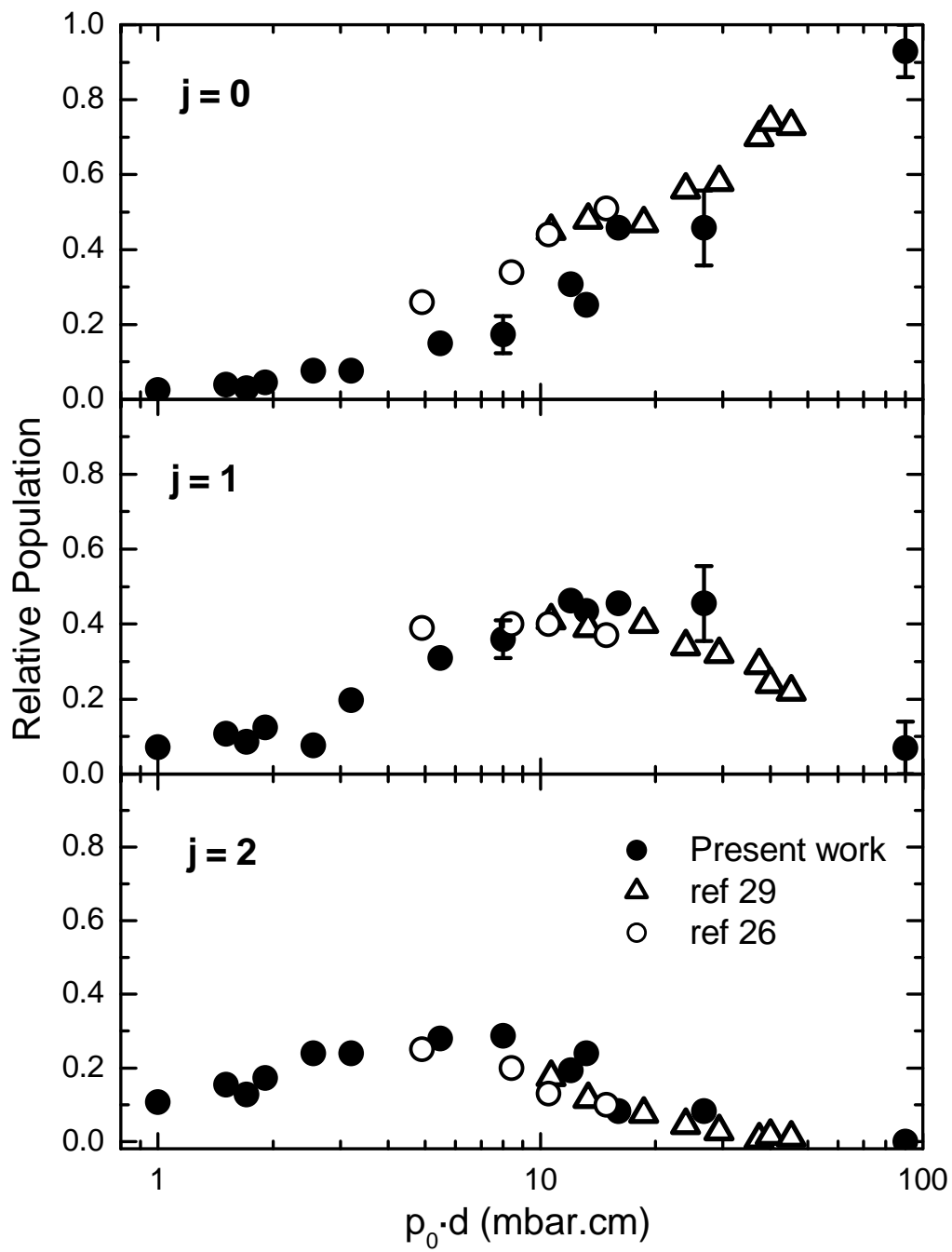
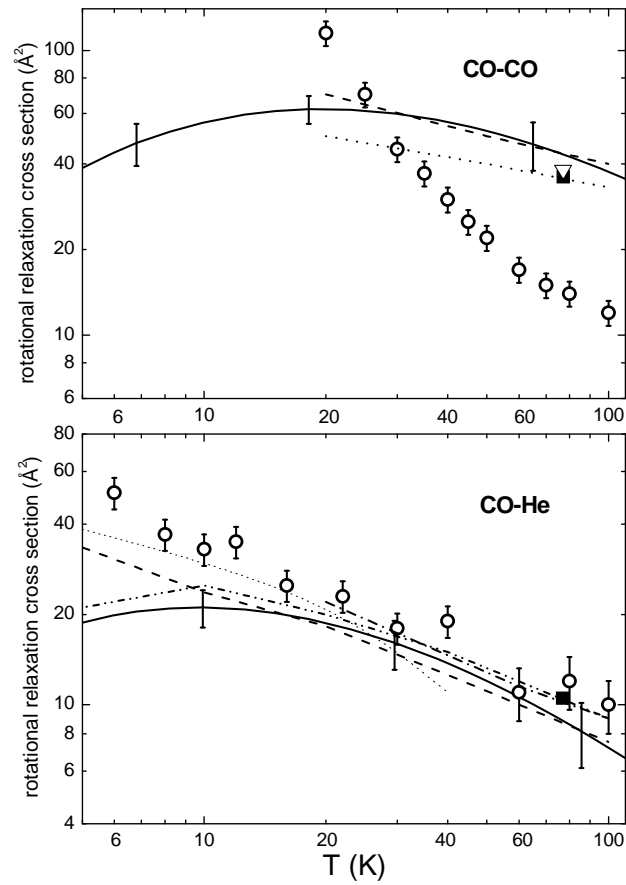


Figure 11 Amaral et al.





**Figure 12** Amaral et al.